

Computational Science Laboratory
Technical Report CSL-TR-00-2013
February 3, 2015

Elias D. Nino, Adrian Sandu and Jeffrey
Anderson

*“An Efficient Implementation of the
Ensemble Kalman Filter Based on an
Iterative Sherman-Morrison Formula”*

Cite as: Elias D. Nino-Ruiz, Adrian Sandu, Jeffrey Anderson, “An efficient implementation of the ensemble Kalman filter based on an iterative ShermanMorrison formula”, *Statistics and Computing*, ISSN: 0960-3174, PP: 1–17, Feb 2014.

Computational Science Laboratory
Computer Science Department
Virginia Polytechnic Institute and State University
Blacksburg, VA 24060
Phone: (540)-231-2193
Fax: (540)-231-6075
Email: enino@vt.edu,sandu@cs.vt.edu
Web: <http://csl.cs.vt.edu>



An Efficient Implementation of the Ensemble Kalman Filter Based on an Iterative Sherman-Morrison Formula

Elias D. Nino[†], Adrian Sandu[†], and Jeffrey Anderson[‡]

[†]Computational Science Laboratory, Department of Computer Science
Virginia Polytechnic Institute and State University

Blacksburg, VA 24060, USA

enino@vt.edu, sandu@cs.vt.edu

[‡]Data Assimilation Research Section

Institute for Mathematics Applied to Geosciences

National Center for Atmospheric Research

Boulder, CO 80307-3000

jala@ucar.edu

Contents

1	Introduction	2
2	Formulation of the EnKF	3
2.1	Efficient implementations of the analysis step	5
3	Iterative Implementation of the EnKF Analysis Step	7
3.1	An iterative Sherman-Morrison formula for matrix inversion	13
3.1.1	Inflation aspects	17
3.1.2	Localization aspects	17
3.2	Computational complexity	18
3.3	Stability Analysis	22
3.4	Pivoting	24
3.5	Parallel implementation	24

4	Experimental Results	27
4.1	Experimental setting	27
4.2	Lorenz-96 model ($N_{\text{ens}} \sim N_{\text{obs}}$)	28
4.3	Quasi-geostrophic model ($N_{\text{obs}} \gg N_{\text{ens}}$)	34
5	Conclusions and Future Work	44

Abstract

We present a practical implementation of the ensemble Kalman (EnKF) filter based on an iterative Sherman-Morrison formula. The new direct method exploits the special structure of the ensemble-estimated error covariance matrices in order to efficiently solve the linear systems involved in the analysis step of the EnKF. The computational complexity of the proposed implementation is equivalent to that of the best EnKF implementations available in the literature when the number of observations is much larger than the number of ensemble members. Even when this condition is not fulfilled, the proposed method is expected to perform well since it does not employ matrix decompositions. Moreover, the proposed method provides the best theoretical complexity when compared to generic formulations of matrix inversion based on the Sherman Morrison formula. The stability analysis of the proposed method is carried out and a pivoting strategy is discussed in order to reduce the accumulation of round-off errors without increasing the computational effort. A parallel implementation is discussed as well. Computational experiments carried out using the Lorenz 96 and then oceanic quasi-geostrophic models reveal that the proposed algorithm yields the same accuracy as other EnKF implementations, but is considerably faster.

Keywords: Ensemble Kalman filter, Matrix Inversion, Sherman-Morrison Formula, Matrix Decomposition

1 Introduction

The ensemble Kalman filter (EnKF) is a well-established, sequential Monte Carlo method to estimate the state and parameters of non-linear, large dynamical models [10] such as those found in atmospheric [22], oil reservoir [9], and oceanic [14] simulations. The popularity of EnKF owes to its simple conceptual formulation and the relative ease implementation [8]. EnKF represents the error statistics by an ensemble of model states, and the evolution of error statistics is obtained implicitly via the time evolution of the ensemble during the forecast step. In the analysis step,

information from the model and the measurements is combined in order to obtain an improved estimate of the true vector state. This process is repeated over the observed time period. In typical data assimilation applications, the dimension of state space (number of variables) ranges between $\mathcal{O}(10^7)$ and $\mathcal{O}(10^9)$, and the dimension of the observation space between $\mathcal{O}(10^5)$ and $\mathcal{O}(10^7)$. Consequently, the dimension of the linear systems solved during the analysis step is very large, and the computational cost considerable. In order to address this challenge we propose an efficient implementation of the EnKF analysis step based on an iterative application of the Sherman-Morrison formula.

The paper is structured as follows. Section 2 discusses the conceptual formulation of the EnKF and several efficient implementations available in the literature. Section 3 presents the novel implementation of the EnKF based on iterative Sherman-Morrison formula, in which the special structure of the measurements error covariance matrix is exploited. Computational cost and stability analyses are carried out for this approach, and pivoting and parallelization ideas are discussed. Section 4 reports numerical results of the proposed algorithm applied to the Lorenz 96 and quasi-geostrophic models. Conclusions are presented in Section 5.

2 Formulation of the EnKF

EnKF consists of two steps: the forecast and the analysis. An EnKF cycle starts with the matrix $\mathbf{X}^B \in \mathbb{R}^{N_{\text{state}} \times N_{\text{ens}}}$ whose columns $\mathbf{x}_i^B \in \mathbb{R}^{N_{\text{state}} \times 1}$ form an ensemble of model states, all corresponding to the same model time t_{current} :

$$\mathbf{X}^B = (\mathbf{x}_1^B, \mathbf{x}_2^B, \dots, \mathbf{x}_{N_{\text{ens}}}^B) \in \mathbb{R}^{N_{\text{state}} \times N_{\text{ens}}}.$$

Typically \mathbf{x}_i^B is an ensemble of model forecasts. Here N_{state} is the size of the model state vector, and N_{ens} is the number of ensemble members. Each ensemble member \mathbf{x}_i^B differs from the true state of the system $\mathbf{x}^{\text{true}} \in \mathbb{R}^{N_{\text{state}} \times 1}$, and we denote by $\xi_i \in \mathbb{R}^{N_{\text{state}} \times 1}$ the corresponding error. The statistics of the ensemble of states is consistent with the background probability distribution.

The ensemble mean $\bar{\mathbf{x}}^B \in \mathbb{R}^{N_{\text{state}} \times 1}$ and the ensemble covariance matrix $\mathbf{P}^B \in \mathbb{R}^{N_{\text{state}} \times N_{\text{state}}}$ can be written as follows:

$$\bar{\mathbf{x}}^B = \frac{1}{N_{\text{ens}}} \sum_{i=1}^{N_{\text{ens}}} \mathbf{x}_i^B = \frac{1}{N_{\text{ens}}} (\mathbf{X}^B \cdot \mathbf{1}_{N_{\text{state}} \times 1}) \in \mathbb{R}^{N_{\text{state}} \times 1}, \quad (1a)$$

$$\bar{\mathbf{X}}^B = \bar{\mathbf{x}}^B \otimes \mathbf{1}_{N_{\text{ens}} \times 1}^T \in \mathbb{R}^{N_{\text{state}} \times N_{\text{ens}}}, \quad (1b)$$

$$\mathbf{P}^B = \frac{1}{N_{\text{ens}} - 1} \cdot (\mathbf{X}^B - \bar{\mathbf{X}}^B) \cdot (\mathbf{X}^B - \bar{\mathbf{X}}^B)^T + \mathbf{Q} \in \mathbb{R}^{N_{\text{state}} \times N_{\text{state}}}. \quad (1c)$$

Here $\mathbf{1}_{N_{\text{ens}} \times 1} \in \mathbb{R}^{N_{\text{ens}} \times 1}$ is a vector whose entries are all equal one. \mathbf{Q} is the covariance matrix of model errors. In the typical case where \mathbf{X}^{B} is an ensemble of model forecasts, the explicit addition of the matrix \mathbf{Q} to the covariance formula is not necessary. Instead, the effect of model errors can be accounted for by adding random vectors $\xi_i \sim \mathcal{N}(0, \mathbf{Q})$ to model states: $\mathbf{x}_i^{\text{B}} \leftarrow \mathbf{x}_i^{\text{B}} + \xi_i$. Prior to any measurement, the forecast step provides the best estimation to the true vector state \mathbf{x}^{true} [28].

The vector of observations $\mathbf{y} \in \mathbb{R}^{N_{\text{obs}} \times 1}$ is available at t_{current} , where N_{obs} is the number of data points. The observations are related to the model state by the relation

$$\mathbf{y} = \mathbf{H} \mathbf{x} + v$$

where $\mathbf{H} \in \mathbb{R}^{N_{\text{obs}} \times N_{\text{state}}}$ is the observation operator which maps the model space state into the observed space, and $v \sim \mathcal{N}(0, \mathbf{R})$ is a vector of observation errors, accounting for both instrument and representativeness errors.

In order to account for observation errors one forms the matrix $\mathbf{Y} \in \mathbb{R}^{N_{\text{obs}} \times N_{\text{ens}}}$ whose columns $\mathbf{y}_i \in \mathbb{R}^{N_{\text{obs}} \times 1}$ are perturbed measurements [15]:

$$\begin{aligned} \mathbf{Y} &= (\mathbf{y} + v_1, \mathbf{y} + v_2, \dots, \mathbf{y} + v_{N_{\text{ens}}}) \\ &= (\mathbf{y}_1, \mathbf{y}_2, \dots, \mathbf{y}_{N_{\text{ens}}}) \in \mathbb{R}^{N_{\text{obs}} \times N_{\text{ens}}}, \end{aligned}$$

The vectors $v_i \in \mathbb{R}^{N_{\text{obs}} \times 1}$ represent errors in the data, and are drawn from a normal distribution $v_i \sim \mathcal{N}(0, \mathbf{R})$. We denote

$$\mathbf{\Upsilon} = (v_1, v_2, \dots, v_{N_{\text{ens}}}) \in \mathbb{R}^{N_{\text{obs}} \times N_{\text{ens}}},$$

and the ensemble representation of the measurements error covariance matrix is

$$\mathbf{R} = \frac{1}{N_{\text{obs}} - 1} \cdot (\mathbf{\Upsilon} \cdot \mathbf{\Upsilon}^{\text{T}}) \in \mathbb{R}^{N_{\text{obs}} \times N_{\text{obs}}}.$$

The EnKF *analysis step* produces an ensemble of improved estimates (analyses) $\mathbf{X}^{\text{A}} \in \mathbb{R}^{N_{\text{state}} \times N_{\text{ens}}}$ by applying the Kalman filter to each of the background ensemble members:

$$\mathbf{X}^{\text{A}} = \mathbf{X}^{\text{B}} + \mathbf{K} \cdot (\mathbf{Y} - \mathbf{H} \cdot \mathbf{X}^{\text{B}}) \in \mathbb{R}^{N_{\text{state}} \times N_{\text{ens}}}, \quad (2a)$$

$$\mathbf{K} = \mathbf{P}^{\text{B}} \cdot \mathbf{H}^{\text{T}} \cdot (\mathbf{H} \cdot \mathbf{P}^{\text{B}} \cdot \mathbf{H}^{\text{T}} + \mathbf{R})^{-1} \in \mathbb{R}^{N_{\text{state}} \times N_{\text{obs}}}, \quad (2b)$$

where the matrix $\mathbf{K} \in \mathbb{R}^{N_{\text{state}} \times N_{\text{obs}}}$ is the Kalman gain and quantifies the contribution of the background–observations difference to the analysis.

The EnKF *forecast step* uses the dynamical model operator \mathcal{M} to evolve each member of the ensemble \mathbf{X}^A from the current time t_{current} to the next time t_{next} where observations are available:

$$\mathbf{X}^B(t_{\text{next}}) = \mathcal{M}_{t_{\text{current}} \rightarrow t_{\text{next}}}(\mathbf{X}^A(t_{\text{current}})) \in \mathbb{R}^{N_{\text{state}} \times N_{\text{ens}}} . \quad (3)$$

The forecast ensemble \mathbf{X}^B is the background for the new EnKF cycle at t_{next} . The analysis and forecast steps are repeated.

2.1 Efficient implementations of the analysis step

From equations (2a)–(2b) the analysis step can be written as

$$\mathbf{X}^A = \mathbf{X}^B + \mathbf{P}^B \cdot \mathbf{H}^T \cdot \mathbf{Z} , \quad (4)$$

where $\mathbf{Z} \in \mathbb{R}^{N_{\text{obs}} \times N_{\text{ens}}}$ is the solution of the following linear system:

$$\underbrace{(\mathbf{H} \cdot \mathbf{P}^B \cdot \mathbf{H}^T + \mathbf{R})}_{\mathbf{W} \in \mathbb{R}^{N_{\text{obs}} \times N_{\text{obs}}}} \cdot \mathbf{Z} = (\mathbf{Y} - \mathbf{H} \cdot \mathbf{X}^B) \in \mathbb{R}^{N_{\text{obs}} \times N_{\text{ens}}} . \quad (5)$$

A direct solution of this linear system can be obtained using the Cholesky decomposition for matrix inversion [17, 26, 31]. While this is a numerically stable and accurate approach [12, 21, 27], its application to (5) leads to the following complexity [19] of the analysis step:

$$\mathcal{O} \left(N_{\text{obs}}^3 + N_{\text{obs}}^2 \cdot N_{\text{ens}} + N_{\text{obs}} \cdot N_{\text{ens}}^2 + N_{\text{state}} \cdot N_{\text{ens}}^2 \right) . \quad (6)$$

This is an acceptable complexity for a large number of degrees of freedom (N_{state}), but not for a large number of observations (N_{obs}). An alternative is to solve (5), and the overall analysis step, using Singular Value Decomposition (SVD) based methods. Those methods exploit the special structure of the data error covariance matrix \mathbf{R} , which is often (block) diagonal and can be easily factorized:

$$\mathbf{R} = \text{diag}(\mathbf{R}_1, \mathbf{R}_2, \dots, \mathbf{R}_{N_{\text{block}}}) , \text{ with } \mathbf{R}_k \in \mathbb{R}^{N_k \times N_k} , 1 \leq k \leq N_{\text{block}} ,$$

where N_{block} is the number of blocks in the matrix \mathbf{R} and:

$$N_{\text{obs}} = \sum_{k=1}^{N_{\text{block}}} N_k .$$

The matrix \mathbf{R} is a covariance matrix, and in practice it is always positive definite.

The observation operator $\mathbf{H} \in \mathbb{R}^{N_{\text{obs}} \times N_{\text{state}}}$ is sparse or can be applied efficiently to a state vector. Then, when \mathbf{R} is diagonal, we can express the system matrix (5) as follows:

$$\begin{aligned}\widehat{\mathbf{S}} &= (\mathbf{X}^{\text{B}} - \overline{\mathbf{X}}^{\text{B}}) \in \mathbb{R}^{N_{\text{state}} \times N_{\text{ens}}}, \\ \mathbf{W} &= \sqrt{\mathbf{R}} \cdot \left[\frac{1}{N_{\text{ens}} - 1} \cdot \sqrt{\mathbf{R}^{-1}} \cdot \mathbf{H} \cdot \widehat{\mathbf{S}} \cdot (\mathbf{H} \cdot \widehat{\mathbf{S}})^{\text{T}} \cdot \sqrt{\mathbf{R}^{-1}} + \mathbf{I} \right] \cdot \sqrt{\mathbf{R}}.\end{aligned}\quad (7)$$

Employ the singular value decomposition

$$\sqrt{\mathbf{R}^{-1}} \cdot \mathbf{H} \cdot \widehat{\mathbf{S}} = \mathbf{U} \cdot \boldsymbol{\Sigma} \cdot \mathbf{V}^{\text{T}} \in \mathbb{R}^{N_{\text{obs}} \times N_{\text{ens}}}, \quad (8)$$

where $\mathbf{U} \in \mathbb{R}^{N_{\text{obs}} \times N_{\text{obs}}}$ and $\mathbf{V} \in \mathbb{R}^{N_{\text{ens}} \times N_{\text{ens}}}$ are orthogonal square matrices, and $\boldsymbol{\Sigma} = \mathbf{diag}(\sigma_1, \sigma_2, \dots, \sigma_{N_{\text{ens}}}) \in \mathbb{R}^{N_{\text{obs}} \times N_{\text{ens}}}$ is the diagonal matrix holding the singular values of $\mathbf{W} \in \mathbb{R}^{N_{\text{obs}} \times N_{\text{obs}}}$. The linear system (5) can be written as follows [19]:

$$\left[\sqrt{\mathbf{R}} \cdot \mathbf{U} \cdot \left(\frac{\boldsymbol{\Sigma}^2}{N_{\text{ens}} - 1} + \mathbf{I} \right) \cdot \mathbf{U}^{\text{T}} \cdot \sqrt{\mathbf{R}} \right] \cdot \mathbf{Z} = (\mathbf{Y} - \mathbf{H} \cdot \mathbf{X}^{\text{B}}) \in \mathbb{R}^{N_{\text{obs}} \times N_{\text{ens}}}, \quad (9)$$

which yields the solution:

$$\mathbf{Z} = \sqrt{\mathbf{R}^{-1}} \cdot \mathbf{U} \cdot \mathbf{diag} \left\{ \left(\frac{\sigma_i^2}{N_{\text{ens}} - 1} + 1 \right)^{-1} \right\} \cdot \mathbf{U}^{\text{T}} \cdot \sqrt{\mathbf{R}^{-1}} \cdot (\mathbf{Y} - \mathbf{H} \cdot \mathbf{X}^{\text{B}}). \quad (10)$$

The overall complexity of the analysis step

$$\mathcal{O} (N_{\text{ens}}^2 \cdot N_{\text{obs}} + N_{\text{ens}}^3 + N_{\text{state}} \cdot N_{\text{ens}}^2) \quad (11)$$

is suitable for large N_{state} and N_{obs} , assuming N_{ens} remains small. Many algorithms in the literature employ SVD (9) for the solution of the linear system (5) [8]. The analysis step is written in terms of the solution (10) in order to minimize the number of matrix computations. Due to this, the solution of the linear system and the improvement of the forecast ensemble are performed as a single step. The ensemble adjustment Kalman filter (EAKF) and the ensemble transform Kalman filter (ETKF) are based on this idea [29]. Other efficient implementations of the ensemble Kalman filter make use of SVD decompositions in order to derive pseudo-inverses, furthermore; these algorithms compute the inverse in the N_{ens} -dimensional ensemble space rather than N_{obs} -dimensional measurement space. Thus, in practice, when $N_{\text{obs}} \gg N_{\text{ens}}$, those algorithms exhibit a good performance. All these methods have the overall complexity (number of long operations) given in (11).

A different approach is to employ iterative methods for solving the linear system (5), for instance the conjugate gradient method [6, 7, 13, 25] for N_{ens} right-hand sides. However, each iteration costs $\mathcal{O}(N_{\text{ens}}^2 \cdot N_{\text{obs}})$, therefore iterative methods do not seem to be competitive for the solution of (5).

The well-established EnKF implementations presented above employ a Cholesky or SVD decomposition, which require considerable computational effort. The next section discusses an efficient implementation of the ensemble Kalman filter which does not require any decomposition prior to the solution of the linear system (5).

3 Iterative Implementation of the EnKF Analysis Step

We make the assumptions [19, 29] that, in practice:

- The data error covariance matrix \mathbf{R} has a simple structure (e.g., is block diagonal).
- The observation operator \mathbf{H} is sparse or can be applied efficiently.
- The variables N_{obs} and N_{state} are very large.

Moreover, we consider the following situations:

- In many real applications of the EnKF $N_{\text{obs}} \gg N_{\text{ens}}$, and the number of variables ranges between $\mathcal{O}(10^7)$ and $\mathcal{O}(10^9)$.
- When many computational resources are available or when the number of components in the model state is relatively small ($N_{\text{state}} \sim \mathcal{O}(10^5)$), the number of ensemble members can be increased considerably in order to provide more accurate statistics. In this case $N_{\text{obs}} \sim N_{\text{ens}}$.

Taking into account the previous assumptions, we now derive the implementation of the EnKF. We define the matrix of member deviations $\mathbf{S} \in \mathbb{R}^{N_{\text{state}} \times N_{\text{ens}}}$ as follows:

$$\mathbf{S} = \frac{1}{\sqrt{N_{\text{ens}} - 1}} \cdot (\mathbf{x}_1^{\text{B}} - \bar{\mathbf{x}}^{\text{B}}, \mathbf{x}_2^{\text{B}} - \bar{\mathbf{x}}^{\text{B}}, \dots, \mathbf{x}_{N_{\text{ens}}}^{\text{B}} - \bar{\mathbf{x}}^{\text{B}}) \in \mathbb{R}^{N_{\text{state}} \times N_{\text{ens}}}, \quad (12)$$

which allows to write the ensemble covariance matrix as

$$\mathbf{P}^{\text{B}} = \mathbf{S} \cdot \mathbf{S}^{\text{T}} \in \mathbb{R}^{N_{\text{state}} \times N_{\text{state}}}. \quad (13)$$

By replacing equation (13) in (5), the linear system solved during the analysis step is written as follows:

$$\mathbf{D} = \mathbf{Y} - \mathbf{H} \cdot \mathbf{X}^B \in \mathbb{R}^{N_{\text{obs}} \times N_{\text{ens}}}, \quad (14a)$$

$$\mathbf{V} = \mathbf{H} \cdot \mathbf{S} \in \mathbb{R}^{N_{\text{obs}} \times N_{\text{ens}}}, \quad (14b)$$

$$(\mathbf{R} + \mathbf{V} \cdot \mathbf{V}^T) \cdot \mathbf{Z} = \mathbf{D} \in \mathbb{R}^{N_{\text{obs}} \times N_{\text{ens}}}. \quad (14c)$$

Note that

$$\mathbf{W} = \mathbf{R} + \mathbf{V} \cdot \mathbf{V}^T = \mathbf{R} + \sum_{i=1}^{N_{\text{ens}}} \mathbf{v}_i \cdot \mathbf{v}_i^T$$

can be computed recursively via the sequence of matrices $\mathbf{W}^{(k)} \in \mathbb{R}^{N_{\text{obs}} \times N_{\text{obs}}}$:

$$\begin{aligned} \mathbf{W}^{(0)} &= \mathbf{R}, \\ \mathbf{W}^{(k)} &= \mathbf{R} + \sum_{i=1}^k \mathbf{v}_i \cdot \mathbf{v}_i^T = \mathbf{W}^{(k-1)} + \mathbf{v}_k \cdot \mathbf{v}_k^T, \quad 1 \leq k \leq N_{\text{ens}}, \end{aligned}$$

therefore

$$\mathbf{W} = \mathbf{W}^{(N_{\text{ens}})} = \mathbf{R} + \sum_{i=1}^{N_{\text{ens}}} \mathbf{v}_i \cdot \mathbf{v}_i^T = \mathbf{W}^{(N_{\text{ens}}-1)} + \mathbf{v}_{N_{\text{ens}}} \cdot \mathbf{v}_{N_{\text{ens}}}^T. \quad (15)$$

By replacing equation (15) in (14c) we obtain:

$$(\mathbf{W}^{(N_{\text{ens}}-1)} + \mathbf{v}_{N_{\text{ens}}} \cdot \mathbf{v}_{N_{\text{ens}}}^T) \cdot \mathbf{Z} = \mathbf{D}. \quad (16)$$

Theorem 3 shows that the matrix (15) is non-singular. The linear system (16) can be solved by making use again of the Sherman-Morrison formula [11]:

$$(\mathbf{A} + \mathbf{L} \cdot \mathbf{M} \cdot \mathbf{N})^{-1} = \mathbf{A}^{-1} - \mathbf{A}^{-1} \cdot \mathbf{L} \cdot (\mathbf{M}^{-1} + \mathbf{N} \cdot \mathbf{A} \cdot \mathbf{L})^{-1} \cdot \mathbf{N} \cdot \mathbf{A}^{-1} \quad (17)$$

with $\mathbf{A} = [\mathbf{W}^{(N_{\text{ens}}-1)}]^{-1}$, $\mathbf{L} = 1$, $\mathbf{M} = \mathbf{v}_{N_{\text{ens}}}$ and $\mathbf{N} = \mathbf{v}_{N_{\text{ens}}}^T$. The solution of (16) is computed as follows:

$$\mathbf{Z} = \mathbf{F}^{(N_{\text{ens}})} - \mathbf{g}^{(N_{\text{ens}})} \cdot (1 + \mathbf{v}_{N_{\text{ens}}}^T \cdot \mathbf{g}^{(N_{\text{ens}})})^{-1} \cdot \mathbf{v}_{N_{\text{ens}}}^T \cdot \mathbf{F}^{(N_{\text{ens}})} \in \mathbb{R}^{N_{\text{obs}} \times N_{\text{ens}}}, \quad (18)$$

where $\mathbf{F}^{(N_{\text{ens}})} \in \mathbb{R}^{N_{\text{obs}} \times N_{\text{ens}}}$ and $\mathbf{g}^{(N_{\text{ens}})} \in \mathbb{R}^{N_{\text{obs}} \times N_{\text{ens}}}$ are given by the solution of the following linear systems:

$$\mathbf{W}^{(N_{\text{ens}}-1)} \cdot \mathbf{F}^{(N_{\text{ens}})} = \mathbf{D} \in \mathbb{R}^{N_{\text{obs}} \times N_{\text{ens}}}, \quad (19a)$$

$$\mathbf{W}^{(N_{\text{ens}}-1)} \cdot \mathbf{g}^{(N_{\text{ens}})} = \mathbf{v}_{N_{\text{ens}}} \in \mathbb{R}^{N_{\text{obs}} \times 1}. \quad (19b)$$

Note that (19a) can be written as follows:

$$\mathbf{W}^{(N_{\text{ens}}-1)} \cdot \mathbf{f}_i^{(N_{\text{ens}})} = \mathbf{d}_i \in \mathbb{R}^{N_{\text{obs}} \times 1}, \quad 1 \leq i \leq N_{\text{ens}}, \quad (20)$$

where $\mathbf{f}_i^{(N_{\text{ens}})} \in \mathbb{R}^{N_{\text{obs}} \times 1}$ and $\mathbf{d}_i \in \mathbb{R}^{N_{\text{obs}} \times 1}$ are the i -th columns of the matrices $\mathbf{F}^{(N_{\text{ens}})}$ and \mathbf{D} , respectively. Following (18), the i -th column of the matrix \mathbf{Z} is given by:

$$\mathbf{z}_i = \mathbf{f}_i^{(N_{\text{ens}})} - \mathbf{g}^{(N_{\text{ens}})} \cdot \left(1 + \mathbf{v}_{N_{\text{ens}}}^{\mathbf{T}} \cdot \mathbf{g}^{(N_{\text{ens}})}\right)^{-1} \cdot \mathbf{v}_{N_{\text{ens}}}^{\mathbf{T}} \cdot \mathbf{f}_i^{(N_{\text{ens}})} \in \mathbb{R}^{N_{\text{obs}} \times 1}. \quad (21)$$

By equation (21), the computation of \mathbf{Z} involves the solution of the linear systems (19b) and (20). We apply the Sherman-Morrison formula (17) again. The solution of the linear system (20) can be obtained as follows:

$$\begin{aligned} \mathbf{f}_i^{(N_{\text{ens}})} &= \mathbf{f}_i^{(N_{\text{ens}}-1)} - \mathbf{g}^{(N_{\text{ens}}-1)} \cdot \left(1 + \mathbf{v}_{N_{\text{ens}}-1}^{\mathbf{T}} \cdot \mathbf{g}^{(N_{\text{ens}}-1)}\right)^{-1} \\ &\quad \cdot \mathbf{v}_{N_{\text{ens}}-1}^{\mathbf{T}} \cdot \mathbf{f}_i^{(N_{\text{ens}}-1)}, \end{aligned} \quad (22)$$

where $\mathbf{f}_i^{(N_{\text{ens}}-1)} \in \mathbb{R}^{N_{\text{obs}} \times 1}$ and $\mathbf{g}^{(N_{\text{ens}}-1)} \in \mathbb{R}^{N_{\text{obs}} \times 1}$ are the solutions of the following linear systems, respectively:

$$\begin{aligned} \mathbf{W}^{(N_{\text{ens}}-2)} \cdot \mathbf{f}_i^{(N_{\text{ens}}-1)} &= \mathbf{d}_i \in \mathbb{R}^{N_{\text{obs}} \times 1}, \\ \mathbf{W}^{(N_{\text{ens}}-2)} \cdot \mathbf{g}^{(N_{\text{ens}}-1)} &= \mathbf{v}_{N_{\text{ens}}-1} \in \mathbb{R}^{N_{\text{obs}} \times 1}. \end{aligned}$$

The linear system (19b) can be solved similarly. Note that the solution of each linear system involves the computation of two new linear systems, derived from the matrix sequence (15). each of the new linear systems can be solved by applying recursively the Sherman-Morrison formula. For simplicity we denote by \mathbf{f} and \mathbf{g} the solutions of the new linear systems in each recursively application of the Sherman-Morrison formula. We have that:

$$\begin{aligned} \mathbf{W}^{(N_{\text{ens}})} \cdot \mathbf{Z} &= \mathbf{D}, \\ [\mathbf{W}^{(N_{\text{ens}})}]^{-1} \cdot \mathbf{d}_i &= \underbrace{[\mathbf{W}^{(N_{\text{ens}}-1)}]^{-1} \cdot \mathbf{d}_i}_{\mathbf{f}} - \underbrace{[\mathbf{W}^{(N_{\text{ens}}-1)}]^{-1} \cdot \mathbf{v}_{N_{\text{ens}}}}_{\mathbf{g}} \\ &\quad \cdot \left(1 + \mathbf{v}_{N_{\text{ens}}}^{\mathbf{T}} \cdot \underbrace{[\mathbf{W}^{(N_{\text{ens}}-1)}]^{-1} \cdot \mathbf{v}_{N_{\text{ens}}}}_{\mathbf{g}}\right)^{-1} \end{aligned}$$

$$\begin{aligned}
& \cdot \mathbf{v}_{N_{\text{ens}}}^{\mathbf{T}} \cdot \underbrace{[\mathbf{W}^{(N_{\text{ens}}-1)}]^{-1} \cdot \mathbf{d}_i}_{\mathbf{f}} \in \mathbb{R}^{N_{\text{obs}} \times 1}, 1 \leq i \leq N_{\text{ens}} \\
[\mathbf{W}^{(N_{\text{ens}}-1)}]^{-1} \cdot \mathbf{d}_i &= \underbrace{[\mathbf{W}^{(N_{\text{ens}}-2)}]^{-1} \cdot \mathbf{d}_i}_{\mathbf{f}} - \underbrace{[\mathbf{W}^{(N_{\text{ens}}-2)}]^{-1} \cdot \mathbf{v}_{N_{\text{ens}}-1}}_{\mathbf{g}} \\
& \cdot \left(1 + \mathbf{v}_{N_{\text{ens}}-1}^{\mathbf{T}} \cdot \underbrace{[\mathbf{W}^{(N_{\text{ens}}-2)}]^{-1} \cdot \mathbf{v}_{N_{\text{ens}}-1}}_{\mathbf{g}} \right)^{-1} \\
& \cdot \mathbf{v}_{N_{\text{ens}}}^{\mathbf{T}} \cdot \underbrace{[\mathbf{W}^{(N_{\text{ens}}-2)}]^{-1} \cdot \mathbf{d}_i}_{\mathbf{f}} \in \mathbb{R}^{N_{\text{obs}} \times 1}, 1 \leq i \leq N_{\text{ens}} \\
[\mathbf{W}^{(N_{\text{ens}}-1)}]^{-1} \cdot \mathbf{v}_{N_{\text{ens}}} &= \underbrace{[\mathbf{W}^{(N_{\text{ens}}-2)}]^{-1} \cdot \mathbf{v}_{N_{\text{ens}}}}_{\mathbf{f}} - \underbrace{[\mathbf{W}^{(N_{\text{ens}}-2)}]^{-1} \cdot \mathbf{v}_{N_{\text{ens}}-1}}_{\mathbf{g}} \\
& \cdot \left(1 + \mathbf{v}_{N_{\text{ens}}-1}^{\mathbf{T}} \cdot \underbrace{[\mathbf{W}^{(N_{\text{ens}}-2)}]^{-1} \cdot \mathbf{v}_{N_{\text{ens}}-1}}_{\mathbf{g}} \right)^{-1} \\
& \cdot \mathbf{v}_{N_{\text{ens}}-1}^{\mathbf{T}} \cdot \underbrace{[\mathbf{W}^{(N_{\text{ens}}-2)}]^{-1} \cdot \mathbf{v}_{N_{\text{ens}}-1}}_{\mathbf{f}} \in \mathbb{R}^{N_{\text{obs}} \times 1}, \\
& \vdots = \vdots \\
[\mathbf{W}^{(k)}]^{-1} \cdot \mathbf{x} &= \underbrace{[\mathbf{W}^{(k-1)}]^{-1} \cdot \mathbf{x}}_{\mathbf{f}} - \underbrace{[\mathbf{W}^{(k-1)}]^{-1} \cdot \mathbf{v}_k}_{\mathbf{g}} \\
& \cdot \left(1 + \mathbf{v}_k^{\mathbf{T}} \cdot \underbrace{[\mathbf{W}^{(k-1)}]^{-1} \cdot \mathbf{v}_k}_{\mathbf{g}} \right)^{-1} \\
& \cdot \mathbf{v}_k^{\mathbf{T}} \cdot \underbrace{[\mathbf{W}^{(k-1)}]^{-1} \cdot \mathbf{x}}_{\mathbf{f}} \in \mathbb{R}^{N_{\text{obs}} \times 1}, \\
[\mathbf{W}^{(k-1)}]^{-1} \cdot \mathbf{x} &= \underbrace{[\mathbf{W}^{(k-2)}]^{-1} \cdot \mathbf{x}}_{\mathbf{f}} - \underbrace{[\mathbf{W}^{(k-2)}]^{-1} \cdot \mathbf{v}_{k-1}}_{\mathbf{g}} \\
& \cdot \left(1 + \mathbf{v}_{k-1}^{\mathbf{T}} \cdot \underbrace{[\mathbf{W}^{(k-2)}]^{-1} \cdot \mathbf{v}_{k-1}}_{\mathbf{g}} \right)^{-1}
\end{aligned}$$

$$\begin{aligned}
& \cdot \mathbf{v}_{k-1}^{\mathbf{T}} \cdot \underbrace{[\mathbf{W}^{(k-1)}]^{-1} \cdot \mathbf{x}}_{\mathbf{f}} \in \mathbb{R}^{N_{\text{obs}} \times 1}, \\
[\mathbf{W}^{(k-1)}]^{-1} \cdot \mathbf{v}_k &= \underbrace{[\mathbf{W}^{(k-2)}]^{-1} \cdot \mathbf{v}_k}_{\mathbf{f}} - \underbrace{[\mathbf{W}^{(k-2)}]^{-1} \cdot \mathbf{v}_{k-1}}_{\mathbf{g}} \\
& \cdot \left(1 + \mathbf{v}_{k-1}^{\mathbf{T}} \cdot \underbrace{[\mathbf{W}^{(k-2)}]^{-1} \cdot \mathbf{v}_{k-1}}_{\mathbf{g}} \right)^{-1} \\
& \cdot \mathbf{v}_{k-1}^{\mathbf{T}} \cdot \underbrace{[\mathbf{W}^{(k-2)}]^{-1} \cdot \mathbf{v}_k}_{\mathbf{f}} \in \mathbb{R}^{N_{\text{obs}} \times 1}, \\
& \vdots = \vdots \\
[\mathbf{W}^{(1)}]^{-1} \cdot \mathbf{x} &= \underbrace{[\mathbf{W}^{(0)}]^{-1} \cdot \mathbf{x}}_{\mathbf{f}} - \underbrace{[\mathbf{W}^{(0)}]^{-1} \cdot \mathbf{v}_1}_{\mathbf{g}} \cdot \left(1 + \mathbf{v}_1^{\mathbf{T}} \cdot \underbrace{[\mathbf{W}^{(0)}]^{-1} \cdot \mathbf{v}_1}_{\mathbf{g}} \right)^{-1} \\
& \cdot \mathbf{v}_1^{\mathbf{T}} \cdot \underbrace{[\mathbf{W}^{(0)}]^{-1} \cdot \mathbf{x}}_{\mathbf{f}}, \\
[\mathbf{W}^{(0)}]^{-1} \cdot \mathbf{x} &= \mathbf{R}^{-1} \cdot \mathbf{x} \in \mathbb{R}^{N_{\text{obs}} \times 1}, \\
[\mathbf{W}^{(0)}]^{-1} \cdot \mathbf{v}_1 &= \mathbf{R}^{-1} \cdot \mathbf{v}_1 \in \mathbb{R}^{N_{\text{obs}} \times 1},
\end{aligned}$$

where $\mathbf{x} \in \mathbb{R}^{N_{\text{obs}} \times 1}$ can be either, a column of matrix $\mathbf{D} \in \mathbb{R}^{N_{\text{obs}} \times N_{\text{ens}}}$ or $\mathbf{V} \in \mathbb{R}^{N_{\text{obs}} \times N_{\text{ens}}}$.

We note that:

- The computation of $[\mathbf{W}^{(k)}]^{-1} \cdot \mathbf{x}$ involves the solution of the linear systems $\mathbf{W}^{(k-1)} \cdot \mathbf{f} = \mathbf{x}$ and $\mathbf{W}^{(k-1)} \cdot \mathbf{g} = \mathbf{v}_k$.
- Since the recursion is based on the sequence of matrices defined in (15), the base case is the linear system $\mathbf{R}^{-1} \cdot \mathbf{x}$ in which the matrix \mathbf{R} is (block) diagonal.

From the previous analysis we derive a recursive Sherman-Morrison formula as follows. Define

$$\mathcal{S}(\mathbf{x}, k) = \begin{cases} \mathbf{z} = \mathbf{R}^{-1} \cdot \mathbf{x}, & \text{for } k = 0, \\ \mathbf{f} = \mathcal{S}(\mathbf{x}, k-1); \\ \mathbf{g} = \mathcal{S}(\mathbf{v}_k, k-1), & \text{for } 1 \leq k \leq N_{\text{ens}}, \\ \mathbf{z} = \mathbf{f} - \mathbf{g} \cdot (1 + \mathbf{v}_k^{\mathbf{T}} \cdot \mathbf{g})^{-1} \cdot \mathbf{v}_k^{\mathbf{T}} \cdot \mathbf{f}; \end{cases} \quad (23)$$

where $\mathbf{x} \in \mathbb{R}^{N_{\text{obs}} \times 1}$. the columns of $\mathbf{Z} \in \mathbb{R}^{N_{\text{obs}} \times N_{\text{ens}}}$ are computed as follows:

$$\mathbf{z}_i = \mathcal{S}(\mathbf{d}_i, N_{\text{ens}}) \in \mathbb{R}^{N_{\text{obs}} \times 1}, \quad 1 \leq i \leq N_{\text{ens}}.$$

The recursive the computations performed by $\mathcal{S}(\bullet)$ can be represented as a tree in which the solution $\mathbf{z} \in \mathbb{R}^{N_{\text{obs}} \times 1}$ of each node depends on the computations of its left ($\mathbf{f} \in \mathbb{R}^{N_{\text{obs}} \times 1}$) and right ($\mathbf{g} \in \mathbb{R}^{N_{\text{obs}} \times 1}$) children (i.e., on the solutions of two linear systems). Figure 1 illustrates the derivation of linear systems in order to solve $\mathbf{W}^{(N_{\text{ens}})} \cdot \mathbf{z} = \mathbf{d}$ for $N_{\text{ens}} = 3$ and $\mathbf{d} \in \{\mathbf{d}_1, \mathbf{d}_2, \mathbf{d}_3\}$, $\mathbf{d} \in \mathbb{R}^{N_{\text{obs}} \times 1}$.

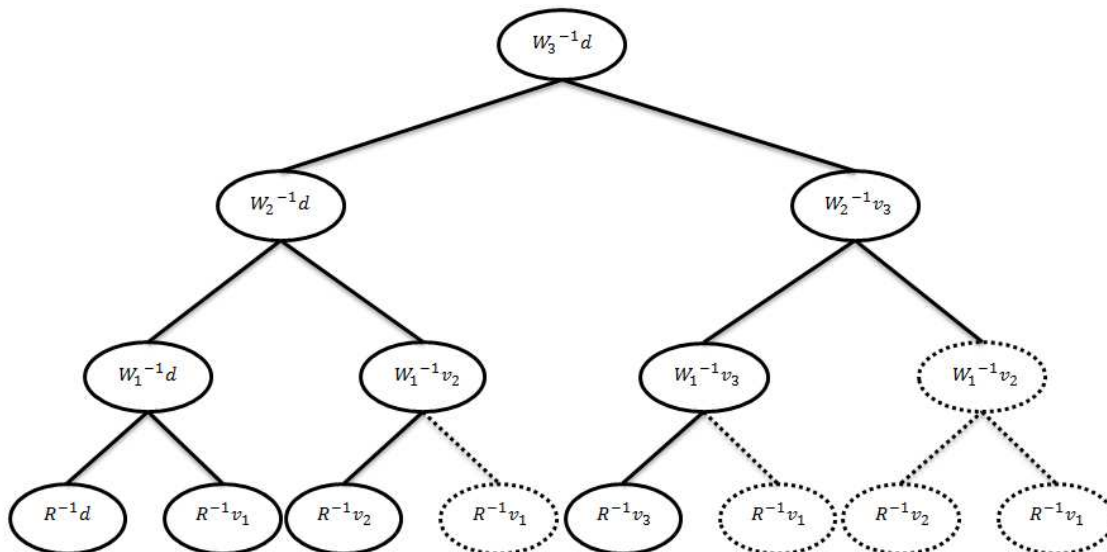


Figure 1: The recursive Sherman-Morrison formula ($\mathcal{S}(\bullet)$) applied to solve the linear system $\mathbf{W}^{(3)} \cdot \mathbf{Z} = \mathbf{D} \in \mathbb{R}^{N_{\text{obs}} \times 3}$. Here \mathbf{d} is any column of matrix $\mathbf{D} \in \mathbb{R}^{N_{\text{obs}} \times 3}$. Dashed nodes represent repeated computations.

We see that $\mathcal{S}(\bullet)$ solves multiple times identical linear systems. For instance, the repeated computations performed in order to solve $\mathbf{W}^{(3)} \cdot \mathbf{Z} = \mathbf{D} \in \mathbb{R}^{N_{\text{obs}} \times 3}$ are represented in Figure 1 as dashed nodes. There, for instance, the linear system $\mathbf{R} \cdot \mathbf{g} = \mathbf{v}_1$ is solved four times in the last level. The total number of linear systems to solve is $\mathcal{O}(N_{\text{ens}} \cdot 2^{N_{\text{ens}}})$, i.e., it increases exponentially with regard to the number of ensemble members if identical computations are not avoided. Next subsection discusses how to achieve this and obtain an efficient implementation of the recursive Sherman-Morrison formula.

3.1 An iterative Sherman-Morrison formula for matrix inversion

In order to avoid identical computations in Figure 1 we can solve the linear systems from the last level of the tree up to the root level. We denote by $\mathbf{U} \in \mathbb{R}^{N_{\text{obs}} \times N_{\text{ens}}}$ and $\mathbf{Z} \in \mathbb{R}^{N_{\text{obs}} \times N_{\text{ens}}}$ the matrices holding partial results of the computations with regard to \mathbf{V} and \mathbf{D} , respectively.

Level 0 can be computed as follows without any repeated effort:

$$\begin{aligned}
\mathbf{U}^{(0)} &= (\mathbf{R}^{-1} \cdot \mathbf{v}_1, \mathbf{R}^{-1} \cdot \mathbf{v}_2, \mathbf{R}^{-1} \cdot \mathbf{v}_3) \\
&= \left([\mathbf{W}^{(0)}]^{-1} \cdot \mathbf{v}_1, [\mathbf{W}^{(0)}]^{-1} \cdot \mathbf{v}_2, [\mathbf{W}^{(0)}]^{-1} \cdot \mathbf{v}_3 \right) \\
&= \left(\mathbf{u}_1^{(0)}, \mathbf{u}_2^{(0)}, \mathbf{u}_3^{(0)} \right), \\
\mathbf{Z}^{(0)} &= (\mathbf{R}^{-1} \cdot \mathbf{d}_1, \mathbf{R}^{-1} \cdot \mathbf{d}_2, \mathbf{R}^{-1} \cdot \mathbf{d}_3) \\
&= \left([\mathbf{W}^{(0)}]^{-1} \cdot \mathbf{d}_1, [\mathbf{W}^{(0)}]^{-1} \cdot \mathbf{d}_2, [\mathbf{W}^{(0)}]^{-1} \cdot \mathbf{d}_3 \right) \\
&= \left(\mathbf{z}_1^{(0)}, \mathbf{z}_2^{(0)}, \mathbf{z}_3^{(0)} \right).
\end{aligned}$$

We make use of the Sherman-Morrison formula (17) and compute level 1 as follows:

$$\begin{aligned}
\mathbf{h}^{(1)} &= \mathbf{u}_1^{(0)} \cdot \frac{1}{1 + \mathbf{v}_1^{\mathbf{T}} \cdot [\mathbf{W}^{(0)}]^{-1} \cdot \mathbf{v}_1} \\
&= \mathbf{u}_1^{(0)} \cdot \frac{1}{1 + \mathbf{v}_1^{\mathbf{T}} \cdot \mathbf{u}_1^{(0)}}, \\
\mathbf{U}^{(1)} &= \left(\mathbf{u}_1^{(0)}, \mathbf{u}_2^{(0)} - \mathbf{h}^{(1)} \cdot \left(\mathbf{v}_1^{\mathbf{T}} \cdot \mathbf{u}_2^{(0)} \right), \mathbf{u}_3^{(0)} - \mathbf{h}^{(1)} \cdot \left(\mathbf{v}_1^{\mathbf{T}} \cdot \mathbf{u}_3^{(0)} \right) \right) \\
&= \left([\mathbf{W}^{(0)}]^{-1} \cdot \mathbf{v}_1, [\mathbf{W}^{(1)}]^{-1} \cdot \mathbf{v}_2, [\mathbf{W}^{(1)}]^{-1} \cdot \mathbf{v}_3 \right) \\
&= \left(\mathbf{u}_1^{(1)}, \mathbf{u}_2^{(1)}, \mathbf{u}_3^{(1)} \right), \\
\mathbf{Z}^{(1)} &= \left(\mathbf{z}_1^{(0)} - \mathbf{h}^{(1)} \cdot \left(\mathbf{v}_1^{\mathbf{T}} \cdot \mathbf{z}_1^{(0)} \right), \mathbf{z}_2^{(0)} - \mathbf{h}^{(1)} \cdot \left(\mathbf{v}_1^{\mathbf{T}} \cdot \mathbf{z}_2^{(0)} \right), \mathbf{z}_3^{(0)} - \mathbf{h}^{(1)} \cdot \left(\mathbf{v}_1^{\mathbf{T}} \cdot \mathbf{z}_3^{(0)} \right) \right) \\
&= \left([\mathbf{W}^{(1)}]^{-1} \cdot \mathbf{d}_1, [\mathbf{W}^{(1)}]^{-1} \cdot \mathbf{d}_2, [\mathbf{W}^{(1)}]^{-1} \cdot \mathbf{d}_3 \right) \\
&= \left(\mathbf{z}_1^{(1)}, \mathbf{z}_2^{(1)}, \mathbf{z}_3^{(1)} \right).
\end{aligned}$$

Note that $\mathbf{u}_1^{(0)}$ has not been updated since it is not needed in the computations of the next levels. Similarly, the computations at level 2 make use of the Sherman-Morrison

formula (17):

$$\begin{aligned}
\mathbf{h}^{(2)} &= \mathbf{u}_2^{(1)} \cdot \frac{1}{1 + \mathbf{v}_2^{\mathbf{T}} \cdot [\mathbf{W}^{(1)}]^{-1} \cdot \mathbf{v}_2} \\
&= \mathbf{u}_2^{(1)} \cdot \frac{1}{1 + \mathbf{v}_2^{\mathbf{T}} \cdot \mathbf{u}_2^{(1)}}, \\
\mathbf{U}^{(2)} &= \left(\mathbf{u}_1^{(1)}, \mathbf{u}_2^{(1)}, \mathbf{u}_3^{(1)} - \mathbf{h}^{(1)} \cdot \left(\mathbf{v}_1^{\mathbf{T}} \cdot \mathbf{u}_3^{(1)} \right) \right) \\
&= \left([\mathbf{W}^{(0)}]^{-1} \cdot \mathbf{v}_1, [\mathbf{W}^{(1)}]^{-1} \cdot \mathbf{v}_2, [\mathbf{W}^{(2)}]^{-1} \cdot \mathbf{v}_3 \right) \\
&= \left(\mathbf{u}_1^{(2)}, \mathbf{u}_2^{(2)}, \mathbf{u}_3^{(2)} \right), \\
\mathbf{Z}^{(2)} &= \left(\mathbf{z}_1^{(1)} - \mathbf{h}^{(2)} \cdot \left(\mathbf{v}_2^{\mathbf{T}} \cdot \mathbf{z}_1^{(1)} \right), \mathbf{z}_2^{(1)} - \mathbf{h}^{(2)} \cdot \left(\mathbf{v}_2^{\mathbf{T}} \cdot \mathbf{z}_2^{(1)} \right), \mathbf{z}_3^{(1)} - \mathbf{h}^{(2)} \cdot \left(\mathbf{v}_2^{\mathbf{T}} \cdot \mathbf{z}_3^{(1)} \right) \right) \\
&= \left([\mathbf{W}^{(2)}]^{-1} \cdot \mathbf{d}_1, [\mathbf{W}^{(2)}]^{-1} \cdot \mathbf{d}_2, [\mathbf{W}^{(2)}]^{-1} \cdot \mathbf{d}_3 \right) \\
&= \left(\mathbf{z}_1^{(2)}, \mathbf{z}_2^{(2)}, \mathbf{z}_3^{(2)} \right).
\end{aligned}$$

The vectors $\mathbf{u}_1^{(1)}$ and $\mathbf{u}_2^{(1)}$ are not required for the computations of level 3, and they are not updated. Making use of the Sherman-Morrison formula (17) once again, the root level is computed as follows:

$$\begin{aligned}
\mathbf{h}^{(3)} &= \mathbf{u}_3^{(1)} \cdot \frac{1}{1 + \mathbf{v}_3^{\mathbf{T}} \cdot \mathbf{W}^{(1)}^{-1} \cdot \mathbf{v}_3} \\
\mathbf{Z}^{(3)} &= \left(\mathbf{z}_1^{(2)} - \mathbf{h}^{(2)} \cdot \left(\mathbf{v}_3^{\mathbf{T}} \cdot \mathbf{z}_1^{(2)} \right), \mathbf{z}_2^{(2)} - \mathbf{h}^{(2)} \cdot \left(\mathbf{v}_3^{\mathbf{T}} \cdot \mathbf{z}_2^{(2)} \right), \mathbf{z}_3^{(2)} - \mathbf{h}^{(2)} \cdot \left(\mathbf{v}_3^{\mathbf{T}} \cdot \mathbf{z}_3^{(2)} \right) \right) \\
&= \left([\mathbf{W}^{(3)}]^{-1} \cdot \mathbf{d}_1, [\mathbf{W}^{(3)}]^{-1} \cdot \mathbf{d}_2, [\mathbf{W}^{(3)}]^{-1} \cdot \mathbf{d}_3 \right) \\
&= [\mathbf{W}^{(3)}]^{-1} \cdot \mathbf{D}.
\end{aligned}$$

The computations performed by this iteration are shown in Figure 2.

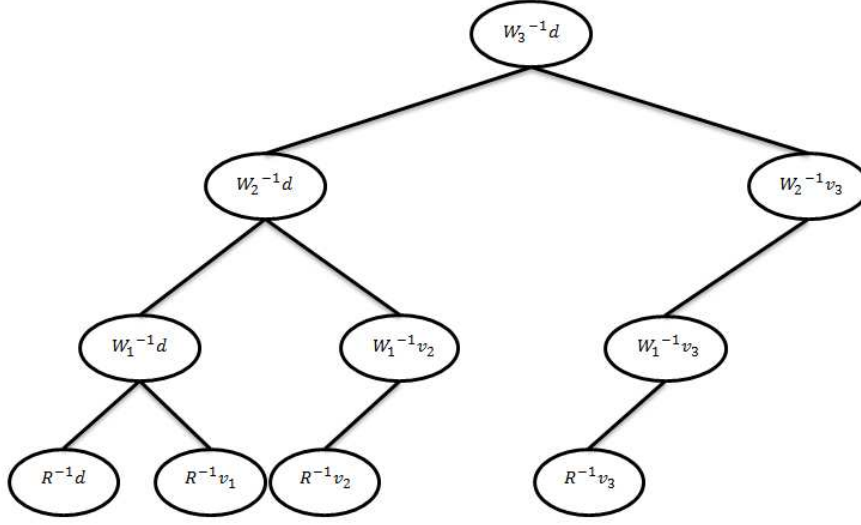


Figure 2: Necessary computations for the solution of $\mathbf{W}^{(3)} \cdot \mathbf{Z} = \mathbf{D} \in \mathbb{R}^{N_{\text{obs}} \times 3}$ using the recursive Sherman-Morrison formula. This iterative version avoids all redundant computations.

Some key features of the iteration are highlighted next.

- The number of iterations is N_{ens} .
- At level 0 matrices $\mathbf{Z}^{(0)}$ and $\mathbf{U}^{(0)}$ are computed as follows:

$$\begin{aligned} \mathbf{Z}^{(0)} &= \mathbf{R}^{-1} \cdot \mathbf{D} \in \mathbb{R}^{N_{\text{obs}} \times N_{\text{ens}}}, \\ \mathbf{U}^{(0)} &= \mathbf{R}^{-1} \cdot \mathbf{V} \in \mathbb{R}^{N_{\text{obs}} \times N_{\text{ens}}}. \end{aligned}$$

- The matrix $\mathbf{W}^{(k)} \in \mathbb{R}^{N_{\text{obs}} \times N_{\text{obs}}}$ is never stored in memory. It can be represented implicitly by matrix $\mathbf{V} \in \mathbb{R}^{N_{\text{obs}} \times N_{\text{ens}}}$. This implicit representation realizes considerable memory savings, especially when $N_{\text{obs}} \gg N_{\text{ens}}$.
- At iteration k , only the columns $\mathbf{u}_i^{(k)}$ with $k < i \leq N_{\text{ens}}$ are updated.

In summary, the solution of the linear system (16) is obtained by the following

iteration:

$$\begin{aligned}
\text{Level 0 : } & \begin{cases} \mathbf{Z}^{(0)} = \mathbf{R}^{-1} \cdot \mathbf{D} \\ \mathbf{U}^{(0)} = \mathbf{R}^{-1} \cdot \mathbf{V} \end{cases} , \\
\text{Level 1 : } & \begin{cases} \mathbf{h}^{(1)} = \left(1 + \mathbf{v}_1^T \cdot \mathbf{u}_1^{(0)}\right)^{-1} \mathbf{u}_1^{(0)} \\ \mathbf{Z}^{(1)} = \mathbf{Z}^{(0)} - \mathbf{h}^{(1)} \cdot \left(\mathbf{v}_1^T \cdot \mathbf{Z}^{(0)}\right) \\ \mathbf{u}_i^{(1)} = \mathbf{u}_i^{(0)} - \mathbf{h}^{(1)} \cdot \left(\mathbf{v}_1^T \cdot \mathbf{u}_i^{(0)}\right) \end{cases} , \quad i = 2, \dots, N_{\text{ens}} \\
& \vdots \\
\text{Level k : } & \begin{cases} \mathbf{h}^{(k)} = \left(1 + \mathbf{v}_k^T \cdot \mathbf{u}_k^{(k-1)}\right)^{-1} \mathbf{u}_k^{(k-1)} \\ \mathbf{Z}^{(k)} = \mathbf{Z}^{(k-1)} - \mathbf{h}^{(k)} \cdot \left(\mathbf{v}_k^T \cdot \mathbf{Z}^{(k-1)}\right) \\ \mathbf{u}_i^{(k)} = \mathbf{u}_i^{(k-1)} - \mathbf{h}^{(k)} \cdot \left(\mathbf{v}_k^T \cdot \mathbf{u}_i^{(k-1)}\right) \end{cases} , \quad i = k + 1, \dots, N_{\text{ens}} \\
& \vdots \\
\text{Level } N_{\text{ens}} : & \begin{cases} \mathbf{h}^{(N_{\text{ens}})} = \left(1 + \mathbf{v}_{N_{\text{ens}}}^T \cdot \mathbf{u}_{N_{\text{ens}}}^{(N_{\text{ens}}-1)}\right)^{-1} \mathbf{u}_{N_{\text{ens}}}^{(N_{\text{ens}}-1)} \\ \mathbf{Z} = \mathbf{Z}^{(N_{\text{ens}})} = \mathbf{Z}^{(N_{\text{ens}}-1)} - \mathbf{h}^{(N_{\text{ens}})} \cdot \left(\mathbf{v}_{N_{\text{ens}}}^T \cdot \mathbf{Z}^{(N_{\text{ens}}-1)}\right) \end{cases} .
\end{aligned}$$

Since the matrix \mathbf{R} has a simple structure its inverse is easy to obtain. In the case of \mathbf{R} (block) diagonal:

$$\mathbf{R}^{-1} = \text{diag} \left(\mathbf{R}^{-1}_1, \mathbf{R}^{-1}_2, \dots, \mathbf{R}^{-1}_{N_{\text{block}}} \right) \in \mathbb{R}^{N_{\text{obs}} \times N_{\text{obs}}},$$

and in general, under the assumptions done (\mathbf{R} is easy to decompose), the computations $\mathbf{Z}^{(0)} = \mathbf{R}^{-1} \cdot \mathbf{D} \in \mathbb{R}^{N_{\text{obs}} \times N_{\text{ens}}}$ and $\mathbf{U}^{(0)} = \mathbf{R}^{-1} \cdot \mathbf{V} \in \mathbb{R}^{N_{\text{obs}} \times N_{\text{ens}}}$ can be performed with no more than $\mathcal{O}(N_{\text{ens}}^2 \cdot N_{\text{obs}})$ long operations.

Putting it all together, we define the iterative Sherman-Morrison formula $\mathcal{S}_\star(\mathbf{R}, \mathbf{V}, \mathbf{D})$ as follows:

- **Step 1.** Compute the matrices $\mathbf{Z}^{(0)} \in \mathbb{R}^{N_{\text{obs}} \times N_{\text{ens}}}$ and $\mathbf{U}^{(0)} \in \mathbb{R}^{N_{\text{obs}} \times N_{\text{ens}}}$ as follows:

$$\mathbf{Z}^{(0)} = \mathbf{R}^{-1} \cdot \mathbf{D}, \quad (24a)$$

$$\mathbf{U}^{(0)} = \mathbf{R}^{-1} \cdot \mathbf{V}, \quad (24b)$$

where \mathbf{R}^{-1} is computed according to its special structure.

- **Step 2.** For $k = 1$ to N_{ens} compute:

$$\mathbf{h}^{(k)} = \left(1 + \mathbf{v}_k^{\mathbf{T}} \cdot \mathbf{u}_k^{(k-1)}\right)^{-1} \mathbf{u}_k^{(k-1)} \in \mathbb{R}^{N_{\text{obs}} \times 1}, \quad (25a)$$

$$\mathbf{Z}^{(k)} = \mathbf{Z}^{(k-1)} - \mathbf{h}^{(k)} \cdot \left(\mathbf{v}_k^{\mathbf{T}} \cdot \mathbf{Z}^{(k-1)}\right) \in \mathbb{R}^{N_{\text{obs}} \times N_{\text{ens}}}, \quad (25b)$$

$$\mathbf{u}_i^{(k)} = \mathbf{u}_i^{(k-1)} - \mathbf{h}^{(k)} \cdot \left(\mathbf{v}_k^{\mathbf{T}} \cdot \mathbf{u}_i^{(k-1)}\right) \in \mathbb{R}^{N_{\text{obs}} \times 1}, \quad k+1 \leq i \leq N_{\text{ens}}. \quad (25c)$$

We now use the iterative Sherman-Morrison formula in the analysis step to obtain an efficient implementation of the Ensemble Kalman filter (SMEnKF). This filter is as follows. The background ensemble states \mathbf{X}^{B} are obtained from the forecast step (3), the ensemble mean $\bar{\mathbf{x}}^{\text{B}}$ is given by (1a), and the ensemble deviations form the mean \mathbf{S} are given by (12). The analysis is obtained as follows:

$$\begin{aligned} \mathbf{D} &= \mathbf{Y} - \mathcal{H}(\mathbf{X}^{\text{B}}) \in \mathbb{R}^{N_{\text{obs}} \times N_{\text{ens}}}, \\ \mathbf{V} &= \mathcal{H}(\mathbf{S}) \in \mathbb{R}^{N_{\text{obs}} \times N_{\text{ens}}}, \\ \mathbf{Z} &= \mathcal{S}_*(\mathbf{R}, \mathbf{V}, \mathbf{D}) \in \mathbb{R}^{N_{\text{obs}} \times N_{\text{ens}}}, \\ \mathbf{X}^{\text{A}} &= \mathbf{X}^{\text{B}} + \mathbf{S} \cdot \mathbf{V}^{\mathbf{T}} \cdot \mathbf{Z} \in \mathbb{R}^{N_{\text{state}} \times N_{\text{ens}}}, \end{aligned}$$

where the function $\mathcal{H}(\mathbf{G}) \in \mathbb{R}^{N_{\text{obs}} \times N_{\text{ens}}}$ is an efficient implementation of the observation operator applied to several state vectors, represented by $\mathbf{G} \in \mathbb{R}^{N_{\text{state}} \times N_{\text{ens}}}$.

3.1.1 Inflation aspects

Inflation increases periodically the ensemble spread, such as to compensate for the small ensemble size, to simulate the existence of model errors, and to avoid filter divergence [16]. All the inflation techniques applied in traditional EnKF can be used, virtually without modification, in the context of SMEnKF. For example, after the forecast step, one can increase the spread of the ensemble

$$\mathbf{x}_i \leftarrow \mathbf{x}_i^{\text{B}} + \alpha (\mathbf{x}_i - \mathbf{x}_i^{\text{B}}), \quad 1 \leq i \leq N_{\text{ens}},$$

such as the ensemble covariance \mathbf{P}^{B} is increased by a factor α^2 [30].

3.1.2 Localization aspects

Using (2b), the analysis step can be written as follows:

$$\begin{aligned} \mathbf{X}^{\text{A}} &= \mathbf{X}^{\text{B}} + \Delta \mathbf{X}^{\text{B}} \\ \Delta \mathbf{X}^{\text{B}} &= \mathbf{S} \cdot \mathbf{V}^{\mathbf{T}} \cdot \mathbf{Z} \\ &= \mathbf{P}^{\text{B}} \cdot \mathbf{H}^{\mathbf{T}} \cdot \left(\mathbf{H} \cdot \mathbf{P}^{\text{B}} \cdot \mathbf{H}^{\mathbf{T}} + \mathbf{R}\right)^{-1} \mathbf{D} \in \mathbb{R}^{N_{\text{state}} \times N_{\text{ens}}} \\ &\approx \mathbf{P}_L^{\text{B}} \cdot \mathbf{H}^{\mathbf{T}} \cdot \left(\mathbf{H} \cdot \mathbf{P}_L^{\text{B}} \cdot \mathbf{H}^{\mathbf{T}} + \mathbf{R}\right)^{-1} \mathbf{D} \in \mathbb{R}^{N_{\text{state}} \times N_{\text{ens}}}. \end{aligned} \quad (26)$$

Localization techniques are explained in detail in [3]. Localization replaces the ensemble based \mathbf{P}^B by a matrix $\mathbf{P}_L^B = \rho \circ \mathbf{P}^B$ in (26), where ρ is a localization matrix and \circ represents the Schur product.

Clearly localization in the form (26) requires the full covariance matrix, and cannot be applied in the context of the iterative Sherman-Morrison implementation. Applying SMEnKF with a single data point \mathbf{y}_i leads to a correction $\Delta \mathbf{X}_{\{i\}}^B$, which can be localized by multiplication with a *diagonal* matrix $\hat{\Delta}_{\{i\}}$ that scales down components with the negative exponential of their distance to the observation i location, and sets them to zero if outside the radius of influence:

$$\Delta \mathbf{X}_{\{i\}}^B = \hat{\Delta}_{\{i\}} \cdot \mathbf{S} \cdot \mathbf{V}^T \cdot \mathbf{Z}_{\{i\}}$$

This can be applied *in succession* for all data points to obtain a fully localized solution.

We discuss next a general approach to perform *partial localization*. Let \mathbf{x}_i be an individual component of the state vector and \mathbf{y}_j an individual observation. Define the impact factor $\delta_{i,j} \in [0, 1]$ of the information in \mathbf{y}_j on the state point \mathbf{x}_i . For example, one can use a correlation length, and a radius about the measurement location outside which the impact factor is zero. Define the influence matrix $\Delta = (\delta_{i,j}) \in \mathbb{R}^{N_{\text{state}} \times N_{\text{obs}}}$, and replace (26) with the following partial localization formula

$$\begin{aligned} \Delta \mathbf{X}^B &\approx \mathbf{P}_L^B \cdot \mathbf{H}^T \cdot (\mathbf{H} \cdot \mathbf{P}^B \cdot \mathbf{H}^T + \mathbf{R})^{-1} \mathbf{d}_\ell \in \mathbb{R}^{N_{\text{state}} \times N_{\text{ens}}} \\ &= \Delta \circ (\mathbf{S} \cdot \mathbf{V}^T) \cdot \mathbf{Z}. \end{aligned}$$

The (i, ℓ) -th entry contains the i -th component the correction vector for the ℓ -th ensemble member and reads

$$\Delta \mathbf{X}_{i,\ell}^B = \sum_{k=1}^{N_{\text{ens}}} \mathbf{S}_{i,k} \sum_{j=1}^{N_{\text{obs}}} \delta_{i,j} \mathbf{V}_{k,j} \mathbf{Z}_{j,\ell}, \quad 1 \leq i \leq N_{\text{state}}, \quad 1 \leq \ell \leq N_{\text{ens}}. \quad (27)$$

The components of the correction matrix (27) are independent of one another, and can be evaluated in parallel after the system solution \mathbf{Z} has been computed.

3.2 Computational complexity

In the complexity analysis of the iterative Sherman-Morrison formula we count only the long operations (multiplications and divisions). Moreover, as discussed before, we make the assumptions presented in [19, 29], namely, the data error covariance matrix $\mathbf{R} \in \mathbb{R}^{N_{\text{obs}} \times N_{\text{obs}}}$ is inexpensive to decompose, and the observation operator \mathbf{H} can

be applied efficiently to any vector. We now analyze each step of the iterative Sherman-Morrison formula when \mathbf{R} is diagonal, the extension to nondiagonal data error covariance matrices is immediate.

In the first step (24) each row i of matrices $\mathbf{D} \in \mathbb{R}^{N_{\text{obs}} \times N_{\text{ens}}}$ and $\mathbf{V} \in \mathbb{R}^{N_{\text{obs}} \times N_{\text{ens}}}$ is divided by the corresponding component $\mathbf{r}_i \in \mathbb{R}^{N_{\text{obs}}}$ in order to obtain $\mathbf{Z}^{(0)} \in \mathbb{R}^{N_{\text{obs}} \times N_{\text{ens}}}$ and $\mathbf{U}^{(0)} \in \mathbb{R}^{N_{\text{obs}} \times N_{\text{ens}}}$ respectively. This yields to $N_{\text{obs}} \cdot N_{\text{ens}}$ number of long operation for each matrix, therefore:

$$T_{\text{step1}}(N_{\text{ens}}, N_{\text{obs}}) = 2 \cdot N_{\text{obs}} \cdot N_{\text{ens}}. \quad (28)$$

In the second step (25) we compute the vector $\mathbf{h}^{(k)} \in \mathbb{R}^{N_{\text{obs}}}$ (25a), and the matrices $\mathbf{Z}^{(k)} \in \mathbb{R}^{N_{\text{obs}} \times N_{\text{ens}}}$ (25b) and $\mathbf{U}^{(k)} \in \mathbb{R}^{N_{\text{obs}} \times N_{\text{ens}}}$ (25c). The number of long operations for each of one are as follows:

$$\begin{aligned} \mathbf{h}^{(k)} &= \mathbf{u}_k^{(k-1)} \cdot \frac{\overbrace{1}^{N_{\text{obs}}}}{1 + \underbrace{\mathbf{v}_k^{\mathbf{T}} \cdot \mathbf{u}_k^{(k-1)}}_{N_{\text{obs}}}}, \\ \mathbf{Z}^{(k)} &= \mathbf{Z}^{(k-1)} - \mathbf{h}^{(k)} \cdot \left(\underbrace{\mathbf{v}_k^{\mathbf{T}} \cdot \mathbf{Z}^{(k-1)}}_{N_{\text{ens}} \cdot N_{\text{obs}}} \right), \\ \mathbf{u}_i^{(k)} &= \mathbf{u}_i^{(k-1)} - \mathbf{h}^{(k)} \cdot \left(\underbrace{\mathbf{v}_k^{\mathbf{T}} \cdot \mathbf{u}_i^{(k-1)}}_{N_{\text{obs}}} \right). \end{aligned}$$

Since the second step (25) is performed N_{ens} times, the number of long operations can be expressed as:

$$\begin{aligned} T_{\text{step2}}(N_{\text{ens}}, N_{\text{obs}}) &= \sum_{k=1}^{N_{\text{ens}}} \left(\underbrace{2 \cdot N_{\text{obs}}}_{\mathbf{h}^{(k)}} + \underbrace{2 \cdot N_{\text{obs}} \cdot N_{\text{ens}}}_{\mathbf{Z}^{(k)}} + \underbrace{\sum_{j=1}^{k-1} (2 \cdot N_{\text{obs}})}_{\mathbf{u}_j^{(k)}} \right) \\ &= 2 \cdot N_{\text{ens}} \cdot N_{\text{obs}} + 2 \cdot N_{\text{ens}}^2 \cdot N_{\text{obs}} + \sum_{k=1}^{N_{\text{ens}}} (k-1) \cdot 2 \cdot N_{\text{obs}} \\ &= 3 \cdot N_{\text{ens}}^2 \cdot N_{\text{obs}} + N_{\text{ens}} \cdot N_{\text{obs}}. \quad (29) \end{aligned}$$

Consequently, from (28)–(29), we have

$$\begin{aligned} T_{\text{SMF}}(N_{\text{ens}}, N_{\text{obs}}) &= \underbrace{2 \cdot N_{\text{obs}} \cdot N_{\text{ens}}}_{T_{\text{step1}}(N_{\text{ens}}, N_{\text{obs}})} + \underbrace{3 \cdot N_{\text{ens}}^2 \cdot N_{\text{obs}} + N_{\text{ens}} \cdot N_{\text{obs}}}_{T_{\text{step2}}(N_{\text{ens}}, N_{\text{obs}})} \\ &= 3 \cdot (N_{\text{ens}}^2 \cdot N_{\text{obs}} + N_{\text{ens}} \cdot N_{\text{obs}}), \end{aligned}$$

which yields a complexity of

$$\mathcal{O}(N_{\text{ens}}^2 \cdot N_{\text{obs}}). \quad (30)$$

Note that when \mathbf{R} is not diagonal, under the assumptions done, the computations (24) of $\mathbf{Z}^{(0)}$ and $\mathbf{U}^{(0)}$ can be efficiently performed in $\mathcal{O}(N_{\text{obs}} \cdot N_{\text{ens}}^2)$ long operations; the overall effort becomes $3 \cdot (N_{\text{ens}}^2 \cdot N_{\text{obs}} + N_{\text{ens}} \cdot N_{\text{obs}})$. This leads to the same complexity (30) for \mathbf{R} diagonal, block diagonal, or in general easy to decompose.

The overall complexity of the analysis step for the iterative formula

$$\mathbf{X}^{\text{A}} = \mathbf{X}^{\text{B}} + \underbrace{\mathbf{S} \cdot \mathbf{V}^{\text{T}} \cdot \underbrace{\mathbf{Z}}_{\mathcal{O}(N_{\text{ens}}^2 \cdot N_{\text{obs}})}}_{\mathcal{O}(N_{\text{ens}}^2 \cdot N_{\text{state}})}$$

is:

$$\mathcal{O}(N_{\text{ens}}^2 \cdot N_{\text{obs}} + N_{\text{ens}}^2 \cdot N_{\text{state}}), \quad (31)$$

The complexity of the proposed implementation of the EnKF is equivalent to the upper bounds of the methods described in [29], as detailed in the Table 1. The term N_{ens}^3 does not appear in the upper-bound of the proposed method even when \mathbf{R} is not diagonal. This term can affect the performance of the EnKF when $N_{\text{ens}} \sim N_{\text{obs}}$.

Analysis method	Computational cost
Direct [29]	$\mathcal{O}(N_{\text{ens}}^2 \cdot N_{\text{obs}} + N_{\text{ens}}^3 + N_{\text{ens}}^2 \cdot N_{\text{state}})$
Serial [4] (for each observation)	$\mathcal{O}(N_{\text{ens}} \cdot N_{\text{obs}} + N_{\text{ens}} \cdot N_{\text{obs}} \cdot N_{\text{state}})$
ETKF [2]	$\mathcal{O}(N_{\text{ens}}^2 \cdot N_{\text{obs}} + N_{\text{ens}}^3 + N_{\text{ens}}^2 \cdot N_{\text{state}})$
EAKF [2]	$\mathcal{O}(N_{\text{ens}}^2 \cdot N_{\text{obs}} + N_{\text{ens}}^3 + N_{\text{ens}}^2 \cdot N_{\text{state}})$
Proposed EnKF Implementation	$\mathcal{O}(N_{\text{ens}}^2 \cdot N_{\text{obs}} + N_{\text{ens}}^2 \cdot N_{\text{state}})$

Table 1: Summary of computational costs of the analysis steps for several ensemble filters. The costs are functions of the ensemble size N_{ens} , number of observations N_{obs} and state dimension N_{state} .

Maponi [20] proposed a general approach based on the Sherman Morrison formula to solve linear systems. The application of this generic algorithm to (16) leads to an increased computational cost as the special structure of the system (and special structure of \mathbf{R}) are not exploited. The generic algorithm applied to EnKF analysis

$$\mathbf{W}^{(N_{\text{ens}})} \mathbf{z}_i = \mathbf{d}_i \in \mathbb{R}^{N_{\text{obs}}}, \text{ for } 1 \leq i \leq N_{\text{ens}}, \quad (32)$$

uses the decomposition [20, Remark 1]:

$$\mathbf{W}^{(N_{\text{ens}})} = \mathbf{W}^{(0)} + \sum_{i=1}^{N_{\text{obs}}} \mathbf{u}_i \cdot \mathbf{v}_i^T,$$

where $\mathbf{W}^{(0)} = \mathbf{diag}(w_1, w_2, \dots, w_{N_{\text{obs}}}) \in \mathbb{R}^{N_{\text{obs}} \times N_{\text{obs}}}$ is a diagonal matrix holding the diagonal entries of $\mathbf{W}^{(N_{\text{ens}})}$, \mathbf{u}_i is the i -th column of $\mathbf{U} = \mathbf{W}^{(N_{\text{ens}})} - \mathbf{W}^{(0)} \in \mathbb{R}^{N_{\text{obs}} \times N_{\text{obs}}}$ and $\mathbf{v}_i = \mathbf{e}_i$ is the i -th element of the canonical basis in $\mathbb{R}^{N_{\text{obs}}}$. Thus, according to [20, Corollary 4], each linear system (32) can be solved with $\mathcal{O}(N_{\text{obs}}^3)$ long operations, leading to a total of

$$\mathcal{O}(N_{\text{ens}} \cdot N_{\text{obs}}^3).$$

Therefore the computational cost of the analysis step is:

$$\mathcal{O}(N_{\text{ens}} \cdot N_{\text{obs}}^3 + N_{\text{ens}} \cdot N_{\text{state}}), \quad (33)$$

which is larger than the computational cost of our proposed EnKF implementation when either $N_{\text{obs}} \gg N_{\text{ens}}$ or $N_{\text{ens}} \sim N_{\text{obs}}$. Moreover, according to [20, Theorem 3], when $N_{\text{obs}} \gg N_{\text{ens}}$, the solution of linear system (32) can be computed with no more than $\mathcal{O}(N_{\text{ens}}^2 \cdot N_{\text{obs}} + N_{\text{ens}}^2)$ long operations. The resulting computational cost of the analysis step is:

$$\mathcal{O}(N_{\text{ens}}^3 \cdot N_{\text{obs}} + N_{\text{ens}}^3 + N_{\text{ens}} \cdot N_{\text{state}}),$$

which is similar to the computational costs of the ETKF and EAKF methods when $N_{\text{obs}} \gg N_{\text{ens}}$. In this case, it is unclear how to construct the matrix $\mathbf{U} \in \mathbb{R}^{N_{\text{obs}} \times N_{\text{ens}}}$ according to Maponi's method; \mathbf{U} can not be chosen as we propose since $\mathbf{W}^{(0)}$ must be diagonal and \mathbf{V} differs from our definition in (14b). In addition, Maponi's algorithm requires the explicit representation in memory of the matrix $\mathbf{W}^{(N_{\text{ens}})}$, which, in practice, is $\mathcal{O}(10^7 \times 10^7)$ dimensional. In contradistinction, $\mathbf{W}^{(N_{\text{ens}})}$ is not required explicitly in memory by our iterative Sherman Morrison formula.

Lastly, the stability conditions of Maponi's method are not discussed in [20]. Furthermore, the sequence of matrices $\mathbf{W}^{(k)}$ are not proved to be non-singular, which is crucial for the well-performance of that method. On the contrary, the stability analysis of the iterative Sherman Morrison formula is discussed in the next section.

3.3 Stability Analysis

The solution of the linear system (5) by the iterative Sherman Morrison formula yields the next sequence of matrices during the computation of $[\mathbf{W}^{(N_{\text{ens}})}]^{-1}$:

$$\begin{aligned} [\mathbf{W}^{(0)}]^{-1} &= \mathbf{R}^{-1} \\ [\mathbf{W}^{(1)}]^{-1} &= \mathbf{R}^{-1} - \frac{1}{\gamma_k} \cdot \mathbf{u}_1^{(0)} \cdot \mathbf{v}_1^T \cdot \mathbf{R}^{-1} = \left(\mathbf{I} - \frac{1}{\gamma_k} \cdot \mathbf{u}_1^{(0)} \cdot \mathbf{v}_1^T \right) [\mathbf{W}^{(0)}]^{-1} \\ &\vdots \\ [\mathbf{W}^{(k)}]^{-1} &= \left(\mathbf{I} - \frac{1}{\gamma_k} \cdot \mathbf{u}_k^{(k-1)} \cdot \mathbf{v}_k^T \right) [\mathbf{W}^{(k-1)}]^{-1} \end{aligned}$$

where

$$\gamma_k = 1 + \mathbf{v}_k^T \cdot \mathbf{u}_k^{(k-1)} \in \mathbb{R}, \text{ for } 1 \leq k \leq N_{\text{ens}}.$$

The following situations may affect the proposed method:

- If any step produces $\gamma_k = 0$, then subsequent steps cannot proceed.
- Round-off errors can be considerably amplified if $\gamma_k \approx 0$ (numerical instability).
- If any matrix $\mathbf{W}^{(k)}$ in the sequence:

$$\{ \mathbf{W}^{(0)}, \mathbf{W}^{(1)}, \dots, \mathbf{W}^{(N_{\text{ens}})} \}, \quad (34)$$

is singular, the algorithm cannot proceed.

We now show that the positive definiteness of the covariance matrix \mathbf{R} is a sufficient in order to guarantee the stability of the iterative Sherman Morrison formula.

Theorem 1. *Assume that \mathbf{R} is positive definite with $\xi^T \mathbf{R} \xi \geq \alpha \|\xi\|^2$ for any $\xi \in \mathbb{R}^{N_{\text{obs}}}$. Then all matrices $\mathbf{W}^{(k)}$ are positive definite with $\xi^T \mathbf{W}^{(k)} \xi \geq \alpha \|\xi\|^2$ for any $\xi \in \mathbb{R}^{N_{\text{obs}}}$.*

Proof. First, $\mathbf{W}^{(0)} = \mathbf{R}$ is positive definite. Next, we proceed by finite induction and assume that $\mathbf{W}^{(k-1)}$ is positive definite with $\xi^T \mathbf{W}^{(k-1)} \xi \geq \alpha \|\xi\|^2$. From (16) we have that:

$$\mathbf{W}^{(k)} = \mathbf{W}^{(k-1)} + \mathbf{v}_k \cdot \mathbf{v}_k^T,$$

and therefore $\mathbf{W}^{(k)}$ is also positive definite:

$$\xi^T \mathbf{W}^{(k)} \xi = \underbrace{\xi^T \mathbf{W}^{(k-1)} \xi}_{\geq \alpha \|\xi\|^2} + \underbrace{(\xi^T \mathbf{v}_k)^2}_{\geq 0} \geq \alpha \|\xi\|^2 \quad \forall \xi \in \mathbb{R}_{\text{obs}}^N.$$

□

Theorem 2. *Assume that \mathbf{R} is positive definite. The sequence of values γ_k generated by the algorithm are strictly greater than one for all $1 \leq k \leq N_{\text{ens}}$.*

Proof. By the iterative Sherman Morrison formula, the common computations ($\mathbf{u}_{k+1}^{(k)}$) are given by:

$$\begin{aligned} \mathbf{u}_1^{(0)} &= \mathbf{R}^{-1} \cdot \mathbf{v}_1 = [\mathbf{W}^{(0)}]^{-1} \cdot \mathbf{v}_1 \\ \mathbf{u}_2^{(1)} &= \underbrace{\left(\mathbf{I} - \frac{1}{\gamma_1} \cdot \mathbf{u}_1^{(0)} \cdot \mathbf{v}_1^T \right) \cdot [\mathbf{W}^{(0)}]^{-1} \cdot \mathbf{v}_2}_{[\mathbf{W}^{(1)}]^{-1}} = [\mathbf{W}^{(1)}]^{-1} \cdot \mathbf{v}_2 \\ &\vdots \\ \mathbf{u}_{k+1}^{(k)} &= \underbrace{\left(\mathbf{I} - \frac{1}{\gamma_k} \cdot \mathbf{u}_k^{(k-1)} \cdot \mathbf{v}_k^T \right) \cdot [\mathbf{W}^{(k-1)}]^{-1} \cdot \mathbf{v}_{k+1}}_{[\mathbf{W}^{(k)}]^{-1}} = [\mathbf{W}^{(k)}]^{-1} \cdot \mathbf{v}_{k+1} \end{aligned} \quad (35)$$

Since $\mathbf{W}^{(k-1)}$ is positive definite we have:

$$\gamma_k = 1 + \mathbf{v}_k^T \cdot \mathbf{u}_k^{(k-1)} = 1 + \underbrace{\mathbf{v}_k^T \cdot [\mathbf{W}^{(k-1)}]^{-1} \cdot \mathbf{v}_k}_{>0} > 1,$$

consequently $\gamma_k > 1$ for all $1 \leq k \leq N_{\text{ens}} - 1$. □

We have the following direct corollary of Theorem 1.

Theorem 3. *Assume that \mathbf{R} is positive definite. At iteration k , the linear system:*

$$\mathbf{W}^{(k)} \cdot \mathbf{Z}^{(k)} = \mathbf{D}, \quad (36)$$

has a unique solution, for $1 \leq k \leq N_{\text{ens}}$.

3.4 Pivoting

Theorem 2 shows that γ_k values cannot be near zero. Due to this, we expect that the round-off errors will not increase considerably during an iteration of the iterative Sherman Morrison formula since:

$$\frac{1}{\gamma_k} \in (0, 1).$$

The following pivoting strategy can be (optionally) applied in order to further decrease round-off error accumulation. It consists of interchanging the columns of matrices \mathbf{V} and $\mathbf{U}^{(k-1)}$ such that the pair $(\mathbf{v}_j, \mathbf{u}_j^{(k-1)})$ maximizes γ_k . Formally, at iteration k , prior the matrix computations (25), we look for a column index i_k such that:

$$i_k = \arg \max_i \left\{ \left| 1 + \mathbf{v}_i^T \cdot \mathbf{u}_i^{(k-1)} \right|, k \leq i \leq N_{\text{ens}} \right\}, \quad (37)$$

and then, the columns k and i_k are interchanged in matrices \mathbf{V} and $\mathbf{U}^{(k-1)}$.

The iterative Sherman Morrison formula with pivoting gives the next computational cost:

$$\begin{aligned} T_{\text{SMF}}^{\text{PIV}}(N_{\text{ens}}, N_{\text{obs}}) &= \underbrace{3 \cdot (N_{\text{ens}}^2 \cdot N_{\text{obs}} + N_{\text{ens}} \cdot N_{\text{obs}})}_{T_{\text{SMF}}(N_{\text{ens}}, N_{\text{obs}})} + \underbrace{\sum_{k=1}^{N_{\text{ens}}} \sum_{i=1}^k N_{\text{obs}}}_{\substack{(37) \\ \text{Pivoting}}}, \\ &= \frac{7}{2} \cdot (N_{\text{ens}}^2 \cdot N_{\text{obs}} + N_{\text{ens}} \cdot N_{\text{obs}}) \end{aligned}$$

which yields to:

$$T_{\text{SMF}}^{\text{PIV}}(N_{\text{ens}}, N_{\text{obs}}) \in \mathcal{O}(N_{\text{ens}}^2 \cdot N_{\text{obs}}),$$

from which we can conclude that seeking the maximum value of γ_k according to (37) does not increase the computational cost of the iterative Sherman Morrison formula. Consequently, the overall complexity in the analysis step remains bounded by (31).

3.5 Parallel implementation

In this section we discuss an efficient parallel implementation of the iterative Sherman-Morrison formula. Since the algorithm (24)–(25) can be applied individually to each

column of the matrices $\mathbf{Z}^{(0)} \in \mathbb{R}^{N_{\text{obs}} \times N_{\text{ens}}}$ and $\mathbf{U}^{(0)} \in \mathbb{R}^{N_{\text{obs}} \times N_{\text{ens}}}$, there are $2 N_{\text{ens}}$ computations that can be performed in parallel. We define the matrix $\mathbf{G}^{(0)} \in \mathbb{R}^{N_{\text{obs}} \times 2 \cdot N_{\text{ens}}}$ holding the columns of $\mathbf{V} \in \mathbb{R}^{N_{\text{obs}} \times N_{\text{ens}}}$ and $\mathbf{D} \in \mathbb{R}^{N_{\text{obs}} \times N_{\text{ens}}}$ as follows:

$$\begin{aligned} \mathbf{G}^{(0)} &= [\mathbf{V}, \mathbf{D}] = [\mathbf{v}_1, \mathbf{v}_2, \dots, \mathbf{v}_{N_{\text{ens}}}, \mathbf{d}_1, \mathbf{d}_2, \dots, \mathbf{d}_{N_{\text{ens}}}], \\ &= \left[\mathbf{g}_1^{(0)}, \dots, \mathbf{g}_{N_{\text{ens}}}^{(0)}, \mathbf{g}_{N_{\text{ens}}+1}^{(0)}, \dots, \mathbf{g}_{2 \cdot N_{\text{ens}}}^{(0)} \right] \in \mathbb{R}^{N_{\text{obs}} \times 2 \cdot N_{\text{ens}}}, \end{aligned} \quad (38)$$

Let N_{proc}^0 be the number of available processors at the initial time. The number of operations per processor is

$$C_{\text{p}}^0 = \frac{2 \cdot N_{\text{ens}}}{N_{\text{proc}}^0}.$$

The matrix (38) can be written as

$$\mathbf{G}^{(0)} = \left[\mathbf{B}_1^{(0)}, \mathbf{B}_2^{(0)}, \dots, \mathbf{B}_{N_{\text{proc}}^0}^{(0)} \right],$$

where the blocks $\mathbf{B}_i^{(0)} \in \mathbb{R}^{N_{\text{obs}} \times C_{\text{p}}^0}$ are

$$\mathbf{B}_i^{(0)} = \left[\mathbf{g}_{(i-1)C_{\text{p}}^0+1}^{(0)}, \mathbf{g}_{(i-1)C_{\text{p}}^0+2}^{(0)}, \dots, \mathbf{g}_{iC_{\text{p}}^0}^{(0)} \right] \in \mathbb{R}^{N_{\text{obs}} \times C_{\text{p}}^0} \text{ for } 1 \leq i \leq N_{\text{proc}}^0,$$

The parallel, first step (24) of the iterative Sherman-Morrison formula is implemented as an update over the blocks:

$$\mathbf{B}_i^{(1)} = \mathbf{R}^{-1} \cdot \mathbf{B}_i^{(0)} \in \mathbb{R}^{N_{\text{obs}} \times C_{\text{p}}^0}, \quad \text{for all } 1 \leq i \leq N_{\text{proc}}^0,$$

which yields

$$\begin{aligned} \mathbf{G}^{(1)} &= \left[\mathbf{R}^{-1} \cdot \mathbf{B}_1^{(0)}, \mathbf{R}^{-1} \cdot \mathbf{B}_2^{(0)}, \dots, \mathbf{R}^{-1} \cdot \mathbf{B}_{N_{\text{proc}}^0}^{(0)} \right] \\ &= \left[\mathbf{B}_1^{(1)}, \mathbf{B}_2^{(1)}, \dots, \mathbf{B}_{N_{\text{proc}}^0}^{(1)} \right] \\ &= \left[\underbrace{\mathbf{g}_1^{(1)}, \dots, \mathbf{g}_{N_{\text{ens}}}^{(1)}}_{\mathbf{U}^{(0)}}, \underbrace{\mathbf{g}_{N_{\text{ens}}+1}^{(1)}, \dots, \mathbf{g}_{2 \cdot N_{\text{ens}}}^{(1)}}_{\mathbf{Z}^{(0)}} \right] \\ &= \left[\mathbf{u}_1^{(0)}, \mathbf{u}_2^{(0)}, \dots, \mathbf{u}_{N_{\text{ens}}}^{(0)}, \mathbf{Z}^{(0)} \right] \end{aligned} \quad (39)$$

The second step (25) of the iterative Sherman-Morrison formula consists of a sequence of updates applied to the matrices $\mathbf{Z}^{(0)}$ and $\mathbf{U}^{(0)}$. Such matrices are represented by the columns of matrix $\mathbf{G}^{(1)}$. Thus, consider the computation of level one, each column of the matrix $\mathbf{G}^{(1)}$ can be updated as follows:

$$\mathbf{g}_i^{(2)} = \mathbf{g}_i^{(1)} - \mathbf{g}_i^{(1)} \cdot \left(\mathbf{1} + \mathbf{v}_1^T \cdot \mathbf{g}_i^{(1)} \right)^{-1} \cdot \left(\mathbf{v}_1^T \cdot \mathbf{g}_i^{(1)} \right) \in \mathbb{R}^{N_{\text{obs}} \times 1}, \quad \mathbf{2} \leq i \leq 2 \cdot N_{\text{ens}}.$$

Similarly to the first step, the computations can be grouped in blocks

$$\mathbf{B}_i^{(1)} = \left[\mathbf{g}_{(i-1)C_p^1+2}^{(1)}, \mathbf{g}_{(i-1)C_p^1+3}^{(1)}, \dots, \mathbf{g}_{iC_p^1+1}^{(1)} \right] \in \mathbb{R}^{N_{\text{obs}} \times C_p^1}, \quad \text{for } 1 \leq i \leq N_{\text{proc}}^1,$$

and distributed over the processors:

$$\mathbf{B}_i^{(2)} = \mathbf{B}_i^{(1)} - \mathbf{g}_1^{(1)} \cdot \left(\mathbf{1} + \mathbf{v}_1^T \cdot \mathbf{g}_1^{(1)} \right)^{-1} \cdot \left(\mathbf{v}_1^T \cdot \mathbf{B}_i^{(1)} \right) \in \mathbb{R}^{N_{\text{obs}} \times C_p^1}, \quad \text{for all } 1 \leq i \leq N_{\text{proc}}^1.$$

Note that $\mathbf{g}_1^{(1)}$ ($\mathbf{u}_1^{(0)}$) is not updated since it is not required in subsequent computations. Thus, for the matrix $\mathbf{G}^{(2)}$

$$\mathbf{G}^{(2)} = \left[\mathbf{g}_1^{(1)}, \mathbf{g}_2^{(2)}, \mathbf{g}_3^{(2)}, \dots, \mathbf{g}_{2 \cdot N_{\text{ens}}}^{(2)} \right],$$

the next common computation is $\mathbf{g}_2^{(2)}$ ($\mathbf{u}_2^{(1)}$), and for the same reasons, this vector is not updated.

In general, at time step t , $1 \leq t \leq N_{\text{ens}}$, the first t columns of the matrix $\mathbf{G}^{(t)}$ are not included in the update process:

$$\mathbf{G}^{(t)} = \left[\mathbf{g}_1^{(1)}, \mathbf{g}_2^{(2)}, \dots, \mathbf{g}_{t-1}^{(t-1)}, \mathbf{g}_t^{(t)}, \mathbf{g}_{t+1}^{(t)}, \dots, \mathbf{g}_{2 \cdot N_{\text{ens}}}^{(t)} \right],$$

The parallel computation of (25) at time step t is performed as follows:

- Compute the number of computation units (columns of matrix $\mathbf{G}^{(t)} \in \mathbb{R}^{N_{\text{obs}} \times N_{\text{ens}}}$) per processor:

$$C_p^t = \frac{2 \cdot N_{\text{ens}} - t}{N_{\text{proc}}^t}.$$

- Perform the update in parallel over the blocks:

$$\mathbf{B}_i^{(t)} = \mathbf{B}_i^{(t)} - \mathbf{g}_t^{(t)} \cdot \left(\mathbf{1} + \mathbf{v}_t^T \cdot \mathbf{g}_t^{(t)} \right)^{-1} \cdot \left(\mathbf{v}_t^T \cdot \mathbf{B}_i^{(t)} \right) \in \mathbb{R}^{N_{\text{obs}} \times C_p^t}, \quad \text{for all } 1 \leq i \leq N_{\text{proc}}^t,$$

where

$$\mathbf{B}_i^{(t)} = \left[\mathbf{g}_{(i-1)C_p^1+1+t}^{(1)}, \mathbf{g}_{(i-1)C_p^1+2+t}^{(1)}, \dots, \mathbf{g}_{iC_p^1+t}^{(1)} \right] \in \mathbb{R}^{N_{\text{obs}} \times C_p^t}.$$

This parallel implementation of the iterative Sherman Morrison formula leads to the complexity:

$$T_{\text{SMF}}^{\text{PAR}}(N_{\text{obs}}, N_{\text{ens}}) = \underbrace{\mathcal{O}(C_p^0 \cdot N_{\text{obs}})}_{\text{step1}} + \sum_{t=1}^{N_{\text{ens}}} \underbrace{\mathcal{O}(C_p^t \cdot N_{\text{obs}})}_{\text{step2}}.$$

Notice, when the number of processors at time $0 \leq t \leq N_{\text{ens}}$ is $N_{\text{proc}}^t = 2 N_{\text{ens}} - t$ then $C_p^t = 1$. Hence, the corresponding computational cost of the analysis step is bounded by:

$$\mathcal{O}(N_{\text{obs}} \cdot N_{\text{ens}} + N_{\text{state}} \cdot N_{\text{ens}}),$$

therefore, when the number of observations is large enough relative to the number of ensemble members, this parallel approach of the iterative Sherman-Morrison formula exhibits a linear behavior, making this implementation attractive.

4 Experimental Results

In this section several computation tests are conducted in order to assess the accuracy and running time of the EnKF based on iterative Sherman Morrison formula.

4.1 Experimental setting

The Sherman-Morrison EnKF implementation as well as the EnKF implementations based on Cholesky and SVD are coded in Fortran 90. The Cholesky and SVD decompositions use functions from the LAPACK library [1] as follows:

- The matrix $\mathbf{W} \in \mathbb{R}^{N_{\text{obs}} \times N_{\text{obs}}}$ is built using DSYRK as follows:

$$\mathbf{W}^{(N_{\text{ens}})} = \alpha \cdot \mathbf{V} \cdot \mathbf{V}^T + \beta \cdot \mathbf{R} \in \mathbb{R}^{N_{\text{obs}} \times N_{\text{obs}}}, \quad \text{with } \alpha = \frac{1}{N_{\text{ens}} - 1}, \quad \beta = 1.0.$$

- The functions DPOTRF and DPOTRI are used to compute the Cholesky decomposition of matrix $\mathbf{W} \in \mathbb{R}^{N_{\text{obs}} \times N_{\text{obs}}}$.
- The SVD decomposition is performed tby the DGESVD function.

In order to measure the quality of the solutions we employ the following performance metrics. The Elapsed Time (ET) measures the overall simulation time for a method $*$. This metric is defined as follows:

$$ET(*) = \text{Forecast}_* + \text{Analysis}_* \quad (40)$$

Where Forecast_* and Analysis_* are the running time for the overall forecast and analysis steps respectively.

The Root Mean Square Error (RMSE) is defined as follows:

$$\varepsilon(*) = \text{RMSE} = \frac{1}{N_{\text{steps}}} \cdot \left(\sum_{t=1}^{N_{\text{steps}}} \text{RSE}_t \right)$$

where N_{steps} is the number of time steps and RSE_t is the Root Square Error at time t defined as follows:

$$\text{RSE}_t = \sqrt{\frac{1}{N_{\text{state}}} \cdot (\mathbf{x}_t^{\text{true}} - \bar{\mathbf{x}}_t^{\text{C}})^{\text{T}} \cdot (\mathbf{x}_t^{\text{true}} - \bar{\mathbf{x}}_t^{\text{C}})}$$

where $\mathbf{x}_t^{\text{true}}$ is the true vector state at time t , and \mathbf{x}_t^{C} can be either the ensemble mean in the forecast $\bar{\mathbf{x}}^{\text{B}}$ or analysis $\bar{\mathbf{x}}^{\text{A}}$ at time t . As can be seen the RMSE measures in average the distance between a reference solution ($\mathbf{x}_t^{\text{true}}$) and the given solution (\mathbf{x}_t^{C}).

The EnKF implementations are tested on two systems: the Lorenz 96 model [18] representing the atmosphere, and a quasi-geostrophic model [5] representing the ocean. They define the model operators (\mathcal{M}) in the EnKF experiments. To compare the performance of different EnKF implementations we measure the elapsed times and the accuracy of analyses for different values of N_{obs} and N_{ens} .

4.2 Lorenz-96 model ($N_{\text{ens}} \sim N_{\text{obs}}$)

The Lorenz 96 model is described by the following system of ordinary differential equations [18]:

$$\frac{d\mathbf{x}_i}{dt} = \begin{cases} (\mathbf{x}_2 - \mathbf{x}_{N_{\text{state}}-1}) \cdot \mathbf{x}_{N_{\text{state}}} - \mathbf{x}_1 + \text{F} & \text{for } i = 1 \\ (\mathbf{x}_{i+1} - \mathbf{x}_{i-2}) \cdot \mathbf{x}_{i-1} - \mathbf{x}_i + \text{F} & \text{for } 2 \leq i \leq N_{\text{state}} - 1, \\ (\mathbf{x}_1 - \mathbf{x}_{N_{\text{state}}-2}) \cdot \mathbf{x}_{N_{\text{state}}-1} - \mathbf{x}_{N_{\text{state}}} + \text{F} & \text{for } i = N_{\text{state}} \end{cases} \quad (41)$$

which has been heuristically formulated in order to take into account properties of global atmospheric models such as the advection, dissipation and forcing. This

model exhibits extended chaos with an external forcing value ($F = 8$), when the solution is in the form of moving waves. For this reason, the model is adequate to perform basic studies of predictability.

The test assesses how the efficiency of the EnKF implementations depend on the input parameters N_{obs} and N_{ens} when $N_{\text{obs}} \sim N_{\text{ens}}$ (the number of observations and ensemble members are relatively close). The experimental setting is described below.

- One time unit of the Lorenz 96 model corresponds to five days of the atmosphere. The observations are made over 500 days (100 time units).
- The background error is assumed to be 5%, i.e., the initial ensemble mean's deviation from the reference solution is drawn from a normal distribution whose standard deviation is 5% of the reference value.
- The external forcing is set to $F = 8.0$.
- The dimensions of the model state are $N_{\text{state}} \in \{500, 1000, 3000, 5000\}$. While the typical dimension for the Lorenz-96 model is $N_{\text{state}} = 40$, we scale the system up to assess the performance of different implementations.
- The number of observations equals the number of states, $N_{\text{obs}} = N_{\text{state}}$. Due to this, the analysis step involves large linear systems of size $\mathbf{W} \in \mathbb{R}^{N_{\text{state}} \times N_{\text{state}}}$.
- The number of ensemble members N_{ens} depends on the size of the state vector as shown in Table 2.
- At each time t , the synthetic observations are constructed as follows:

$$\mathbf{y}_t = \mathbf{x}_t^{\text{true}} + v_t \in \mathbb{R}^{N_{\text{state}}} \quad (42)$$

since the number of observations and variables of the vector state are the same. v_t belongs to a normal distribution with zero mean and covariance matrix

$$\mathbf{R} = \mathbf{diag} \{0.01^2\} \in \mathbb{R}^{N_{\text{state}} \times N_{\text{state}}},$$

as is usual in practice. The errors are replicated for each compared, EnKF implementation. Due to this, the same data errors are hold for all tests.

- The assimilation window is five model days.

- The localization (27) is applied using the influence factors

$$\delta_{i,j} = \exp\left(-\frac{\min\{i,j\}}{N_{\text{state}}}\right) \in \mathbb{R}^{N_{\text{state}} \times N_{\text{ens}}}$$

where $\min\{i,j\}$ is the minimum distance between the indexes i and j of the vector state; this distance accounts for the periodic boundary conditions in (41).

The RMSE results are shown in Table 3. All methods provide virtually identical analyses. As expected, the analysis improves when the size of the ensemble is increased.

N_{state}	N_{ens}
500	{200,250,300,350,400}
1000	{400,450,500,550,600}
3000	{900,950,1000,1050,1100}
5000	{1500,1550,1600}

Table 2: Number of ensemble members N_{ens} with respect to the dimension of the vector state N_{state} .

N_{state}/N_{obs}	Step	N_{ens}	EnKF _{Sher}	EnKF _{Chol}	EnKF _{SVD}
500/500	Forecast	200	0.006491846885685	0.006491846885685	0.006491846885685
		250	0.003089844737585	0.003089844737585	0.003089844737585
		300	0.001923620680204	0.001923620680204	0.001923620680204
		350	0.001501324727984	0.001501324727984	0.001501324727984
		400	0.001238879857327	0.001238879857327	0.001238879857327
	Analysis	200	0.005406046859821	0.005406046859821	0.005406046859821
		250	0.002577923867043	0.002577923867043	0.002577923867043
		300	0.001595214779293	0.001595214779293	0.001595214779293
		350	0.001239247824936	0.001239247824936	0.001239247824936
		400	0.001019599347515	0.001019599347515	0.001019599347515
1000/1000	Forecast	400	0.004416601672762	0.004416601672762	0.004416601672762
		450	0.002808556499338	0.002808556499338	0.002808556499338
		500	0.002256025116209	0.002256025116209	0.002256025116209
		550	0.001827747641793	0.001827747641793	0.001827747641793
		600	0.001561032221877	0.001561032221877	0.001561032221877
	Analysis	400	0.003643849246395	0.003643849246395	0.003643849246395
		450	0.002320171220995	0.002320171220995	0.002320171220995
		500	0.001863322297334	0.001863322297334	0.001863322297334
		550	0.001503808242092	0.001503808242092	0.001503808242092
		600	0.001281928557481	0.001281928557481	0.001281928557481
3000/3000	Forecast	900	0.009439626047886	0.009439626047886	0.009439626047886
		950	0.007199551317193	0.007199551317193	0.007199551317193
		1000	0.005410752525373	0.005410752525373	0.005410752525373
		1050	0.004299142614958	0.004299142614958	0.004299142614958
		1100	0.003476460994219	0.003476460994219	0.003476460994219
	Analysis	900	0.007957954481050	0.007957954481050	0.007957954481050
		950	0.006074278547494	0.006074278547494	0.006074278547494
		1000	0.004552394986586	0.004552394986586	0.004552394986586
		1050	0.003597428757064	0.003597428757064	0.003597428757064
		1100	0.002902565379165	0.002902565379165	0.002902565379165
5000/5000	Forecast	1500	0.007678111830765	0.007678111830765	0.007678111830765
		1550	0.006378636076218	0.006378636076218	0.006378636076218
		1600	0.005608079561230	0.005608079561230	0.005608079561230
	Analysis	1500	0.006490749509210	0.006490749509210	0.006490749509210
		1550	0.005389012789042	0.005389012789042	0.005389012789042
		1600	0.004728980886456	0.004728980886456	0.004728980886456

Table 3: RMSE for the Lorenz-96 model with different number of states. When the number of ensemble members is increased the estimation of the true vector state is improved. All EnKF implementations provide virtually identical results.

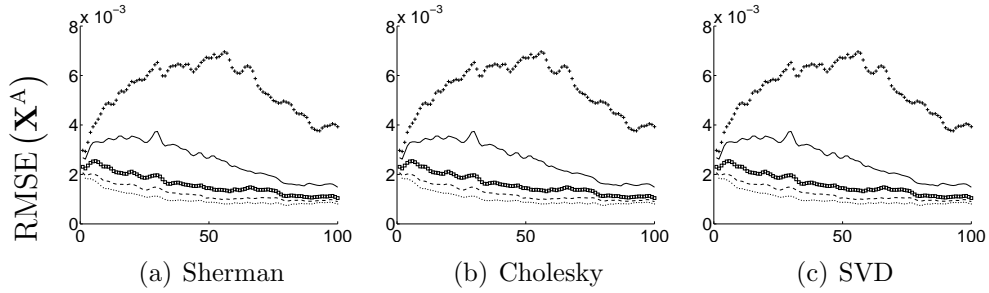


Figure 3: Analysis RMSE for the Lorenz model with 500 of variables. Different curves correspond to different numbers of ensemble members: 200(+), 250(-), 300(\square), 350(---) and 400(.). When the number of ensemble members is increased the analysis is improved.

Figures 3 and 4 show the RMSE decrease over the assimilation window for $N_{\text{state}} = 500$ and 1000, respectively. When the number of ensemble members is increased the analysis errors are smaller, as expected. There is no significant difference in results between different implementations of the EnKF.

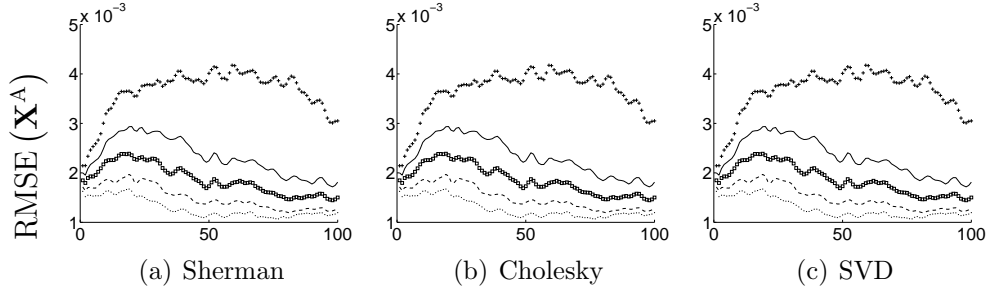


Figure 4: Analysis RMSE for the Lorenz model with 1000 of variables. Different curves correspond to different numbers of ensemble members: 200(+), 250(-), 300(\square), 350(---) and 400(.). When the number of ensemble members is increased the analysis is improved.

The ET results are shown in Table 4. The Cholesky decomposition is the most efficient for a small number of observations and states. When the number of observations is increased, the relative performance of Cholesky deteriorates, as expected from the complexity results presented in Section 1. The Cholesky decomposition solution of the linear system (5) is not suitable when the number of observations is large. The SVD implementation exhibits a good performance for a small number

of ensemble members and observations. However, the ET of the SVD implementation grows faster than that of the Cholesky implementation when the number of ensemble and/or observations are increased, due to the term $N_{\text{ens}}^3 \sim N_{\text{obs}}^3$ in its complexity formula. The EnKF implementation based on SVD is not suitable for a large number of observations or a large number of ensemble members. Finally, the Sherman-Morrison implementation has the best performance for a large number of observations and states. This implementation is suitable for a large number of observations. Since the term N_{ens}^3 does not appear in the cost upper-bound of the iterative-Sherman implementation, when $N_{\text{ens}} \sim N_{\text{obs}}$, the proposed implementation will exhibit a better performance than those implementations presented in [2, 4, 29] since they are upper-bounded by (11) (see table 1).

$N_{\text{obs}}/N_{\text{state}}$	N_{ens}	EnKF_{Sher}	EnKF_{Chol}	EnKF_{SVD}
500/500	200	46.5 s	36.9 s	66.3 s
	250	72.1 s	45.1 s	91.4 s
	300	103.5 s	54.2 s	118.9 s
	350	140.8 s	64.4 s	138.8 s
	400	183.6 s	75.4 s	174.5 s
1000/1000	400	377.6 s	327.4 s	687.1 s
	450	500.1 s	364.6 s	715.9 s
	500	601.7 s	403.5 s	877.3 s
	550	731.8 s	462.4 s	1038.3 s
	600	873.2 s	492.4 s	1199.3 s
3000/3000	900	1.7 h	2.3 h	3.8 h
	950	2.1 h	2.4 h	3.9 h
	1000	2.2 h	2.5 h	4.1 h
	1050	2.4 h	2.7 h	4.4 h
	1100	2.6 h	2.8 h	4.8 h
5000/5000	1500	8.1 h	11.0 h	17.3 h
	1550	8.8 h	11.2 h	17.8 h
	1600	9.2 h	11.5 h	19.9 h

Table 4: Computational times for the Lorenz model assimilation performed with different EnKF implementations. The Cholesky decomposition is the most efficient for a small number of observations and states. The Sherman-Morrison implementation is the bet for a large number of observations and states.

4.3 Quasi-geostrophic model ($N_{\text{obs}} \gg N_{\text{ens}}$)

The Earth's ocean has a complex flow system influenced by the rotation of the Earth, the density stratification due to temperature and salinity, as well as other factors. The quasi-geostrophic (QG) model is a simple model which mimics the real behavior of the ocean. It is defined by the following partial differential equations [5]:

$$\frac{\partial q}{\partial t} + r \cdot \mathcal{J}(\psi, q) + \beta \cdot \frac{\partial \psi}{\partial x} = -rkb \cdot \zeta + rkh \cdot \nabla^2 \zeta - rkh2 \cdot \nabla^4 \zeta + \underbrace{\sin(2 \cdot \pi \cdot y)}_{\text{External Force}}, \quad (43)$$

where

$$\mathcal{J}(\psi, q) = \frac{\partial q}{\partial x} \cdot \frac{\partial \psi}{\partial y} - \frac{\partial q}{\partial y} \cdot \frac{\partial \psi}{\partial x}, \quad (44)$$

$q = \zeta - F \cdot \psi$ is the potential vorticity, ψ is the stream function, F is the Froud number, $\zeta = \nabla^2 \psi$ is the relative vorticity, r is a sort of the Rossby number, rkb is the bottom friction, rkh is the horizontal friction and $rkh2$ is the biharmonic horizontal friction and x and y represent the horizontal and vertical components of the space.

Moreover, q and ψ are related to one another through an elliptic operator [24]:

$$q = \tilde{\nabla}^2 \psi, \quad (45)$$

which yields

$$\tilde{\nabla}^{-2} q = \psi, \quad (46)$$

where

$$\tilde{\nabla}^2 = \frac{\partial^2}{\partial x^2} + \frac{\partial^2}{\partial y^2}.$$

This elliptic property reflects the assumption that the flow is geostrophically balanced in the horizontal direction, and hydrostatically balanced in the vertical direction.

The QG experiment studies the behavior of EnKF implementations when $N_{\text{obs}} \gg N_{\text{ens}}$ (the number of observations is much larger than the number of ensemble members) as is usually the case in practice. Moreover, this scenario is more difficult than the previous one (the Lorenz model): large model-errors are considered in the initial ensemble members. Besides, data is available every 10 time units.

We consider three different grids, denoted QGNM, where the number of horizontal and vertical grid points are N and M , respectively. Specifically, we employ in experiments QG33 (small instance), QG65 (medium instance) and QG129 (large instance). The horizontal and vertical dimensions of the grid are denoted by L_x and L_y respectively. These instances and the corresponding parameter values are summarized in Table 5.

Instance	L_x	L_y	N	M	rkb	rkh	rkh2	β	r
QG33	0.4	0.4	33	33	10^{-6}	10^{-7}	2×10^{-12}	1.0	10^{-5}
QG65	1.0	1.0	65	65	10^{-6}	10^{-7}	2×10^{-12}	1.0	10^{-5}
QG129	1.0	1.0	129	129	10^{-6}	10^{-7}	2×10^{-12}	1.0	10^{-5}

Table 5: Parameter values for the QG model instances considered. L_x and L_y represent the horizontal and vertical grid sizes, and N and M are the number of horizontal and vertical grid points, respectively.

The experimental settings are described below.

- There are 1200 time steps, each of one representing 1.27 days in the ocean.
- The vorticity of the ocean at each grid point provides a component of the vector state.
- The computation of the stream function is done through the solution of the Helmholtz [23] function according to the elliptic property (46).
- Homogeneous Dirichlet boundary conditions are assumed. Due to this, the boundaries of the grid are not mapped into the state vector, and $N_{\text{state}} = (N - 2) \cdot (M - 2)$.
- The initial ensemble members are constructed as follows:

$$\mathbf{x}_i^B = \mathbf{x}^{\text{true}} + \varepsilon_i^B \cdot \underbrace{\left(\frac{1}{N_{\text{state}}} \cdot \sum_{k=1}^{N_{\text{state}}} |\mathbf{x}_k^{\text{true}}| \right)}_{\mathbf{C}} \in \mathbb{R}^{N_{\text{state}} \times 1}, \text{ for } 1 \leq i \leq N_{\text{ens}},$$

where ε_i^B is drawn from a Normal distribution with zero mean and covariance matrix

$$\mathbf{Q} = \text{diag} \{ \text{STD}_{\text{ens}}^2 \} \in \mathbb{R}^{N_{\text{state}} \times N_{\text{state}}}.$$

For testing purposes, three values are assumed for the standard deviation of model errors (STD_{ens}): 2.5, 5.0 and 7.5. Notice the large dispersion of the initial ensemble members, which can make difficult the convergence of any filter since the huge spread out of the initial ensemble members with respect to the typical value \mathbf{C} .

- The number of observation per simulation, for each size (N_{state}) of the model state, is defined as follows:

$$N_{\text{obs}} = P_{\text{obs}} \cdot N_{\text{state}},$$

where P_{obs} is the percentage of components observed from the model state. The values given to P_{obs} are 50%, 70% and 90%. Those, measurements are taken every 10 time units and they are constructed as shown in equation (42). Notice, there are 120 analysis steps out of 1200 time steps (10% of the total simulation time).

- For the time evolution of the model, zero boundary conditions are assumed and the boundaries are not included onto the ensemble representation. Due to this, the dimension of the vector state $N_{\text{state}} = (N - 2) \cdot (M - 2)$.
- For each instance we consider simulations with $N_{\text{ens}} \in \{20, 60, 100\}$ ensemble members. The number of ensemble members is one to two orders of magnitude smaller than the total number of observations.

The RSME values for analysis errors for the QG33, QG65 and QG129 instances are shown in Tables 6, 8 and 10, respectively. The results depend on the number of ensemble members (N_{ens}), the number of observations (N_{obs}), and the deviation of the initial ensemble mean (STD_{ens}). The RSME is quantifies errors in the stream function ψ , whose values are computed through the relation (46). In terms of accuracy there is no significant difference between different EnKF implementations. As expected, when the error in the initial ensemble is increased, the accuracy in the analysis decreases. The error does not show an exponential growth, even when the number of components in the model state (N_{state}) is much larger than the number of ensemble members (e.g., for the QG129 instance). When the number of ensemble members is increased, the analysis error is decreased. This is illustrated by the snapshots of the QG33 simulation over 1200 time steps presented in Figure 5. There, we can clearly see that the ensemble of size 100 provides a better estimation ($\bar{\mathbf{x}}^{\text{B}}$) to the true state of the model (\mathbf{x}^{true}) than the ensembles of sizes 20 and 60. Additionally, the number of observations plays an important role in the estimation of the true

model state when the size of the vector state is much larger than the number of ensemble members.

The ET values for the QG33, QG65 and QG129 simulations are shown in Tables 6, 8 and 10, respectively. The time is expressed in seconds (s) if it is below 30 minutes, and otherwise is expressed in minutes (min) and hours (h). The Cholesky implementation shows good performance when the number of observations is small. From Table 7 (the blocks where the number of observations are 480, 672 and 864) we see that the Cholesky implementation performance is more sensitive to the number of observations than to the number of ensemble members. This EnKF implementation is not suitable for a large number of observations. For instance, the Cholesky elapsed time for the QG129 instance is not presented since each simulation takes more than 4 days in order to be completed.

The SVD implementation shows a better relative performance than for the Lorenz 96 test, since the number of ensemble members is small with respect to the number of observations. For example, for the QG33 instance, the SVD implementation shows a better performance than Cholesky when the number of observations and ensemble members are small. In addition, when the size of vector state is increased, the SVD implementation shows a better performance than Cholesky. This agrees with the computational complexity upper bounds presented in Section 1. As is expected, the performance of the SVD based methods is better than the Cholesky implementations when the number of observations is much larger than the number of the ensemble members.

The Sherman-Morrison implementation shows the best performance among the compared methods. This is true even when the number of observations is much larger than the number of ensemble members, as seen in Table 11. The results of both test cases (the quasigeostrophic and Lorenz models) lead to the conclusion that the performance of the iterative-Sherman implementation is not sensitive to the increase in the number of observations, making it attractive for implementation with large-scale observational systems.

N_{ens}	N_{obs}	STD_{ens}	$\text{EnKF}_{\text{Sher}}$	$\text{EnKF}_{\text{Chol}}$	EnKF_{SVD}
20	480	2.5	$1.71348538 \times 10^{-4}$	$1.71348538 \times 10^{-4}$	$1.71348538 \times 10^{-4}$
		5.0	$3.42503478 \times 10^{-4}$	$3.42503478 \times 10^{-4}$	$3.42503478 \times 10^{-4}$
		7.5	$5.13685273 \times 10^{-4}$	$5.13685273 \times 10^{-4}$	$5.13685273 \times 10^{-4}$
	672	2.5	$1.68916683 \times 10^{-4}$	$1.68916683 \times 10^{-4}$	$1.68916683 \times 10^{-4}$
		5.0	$3.37557073 \times 10^{-4}$	$3.37557073 \times 10^{-4}$	$3.37557073 \times 10^{-4}$
		7.5	$5.06204927 \times 10^{-4}$	$5.06204927 \times 10^{-4}$	$5.06204927 \times 10^{-4}$
	864	2.5	$1.68758284 \times 10^{-4}$	$1.68758284 \times 10^{-4}$	$1.68758284 \times 10^{-4}$
		5.0	$3.37604000 \times 10^{-4}$	$3.37604000 \times 10^{-4}$	$3.37604000 \times 10^{-4}$
		7.5	$5.06437992 \times 10^{-4}$	$5.06437992 \times 10^{-4}$	$5.06437992 \times 10^{-4}$
60	480	2.5	$1.71410180 \times 10^{-4}$	$1.71410180 \times 10^{-4}$	$1.71410180 \times 10^{-4}$
		5.0	$3.43004244 \times 10^{-4}$	$3.43004244 \times 10^{-4}$	$3.43004244 \times 10^{-4}$
		7.5	$5.14603943 \times 10^{-4}$	$5.14603943 \times 10^{-4}$	$5.14603943 \times 10^{-4}$
	672	2.5	$1.64430970 \times 10^{-4}$	$1.64430970 \times 10^{-4}$	$1.64430970 \times 10^{-4}$
		5.0	$3.29692664 \times 10^{-4}$	$3.29692664 \times 10^{-4}$	$3.29692664 \times 10^{-4}$
		7.5	$4.94948120 \times 10^{-4}$	$4.94948120 \times 10^{-4}$	$4.94948120 \times 10^{-4}$
	864	2.5	$1.64737541 \times 10^{-4}$	$1.64737541 \times 10^{-4}$	$1.64737541 \times 10^{-4}$
		5.0	$3.29861914 \times 10^{-4}$	$3.29861914 \times 10^{-4}$	$3.29861914 \times 10^{-4}$
		7.5	$4.94925540 \times 10^{-4}$	$4.94925540 \times 10^{-4}$	$4.94925540 \times 10^{-4}$
100	480	2.5	$1.62358824 \times 10^{-4}$	$1.62358824 \times 10^{-4}$	$1.62358824 \times 10^{-4}$
		5.0	$3.23304631 \times 10^{-4}$	$3.23304631 \times 10^{-4}$	$3.23304631 \times 10^{-4}$
		7.5	$4.84328422 \times 10^{-4}$	$4.84328422 \times 10^{-4}$	$4.84328422 \times 10^{-4}$
	672	2.5	$1.54859388 \times 10^{-4}$	$1.54859388 \times 10^{-4}$	$1.54859388 \times 10^{-4}$
		5.0	$3.10925745 \times 10^{-4}$	$3.10925745 \times 10^{-4}$	$3.10925745 \times 10^{-4}$
		7.5	$4.66772642 \times 10^{-4}$	$4.66772642 \times 10^{-4}$	$4.66772642 \times 10^{-4}$
	864	2.5	$1.44950729 \times 10^{-4}$	$1.44950729 \times 10^{-4}$	$1.44950729 \times 10^{-4}$
		5.0	$2.90313729 \times 10^{-4}$	$2.90313729 \times 10^{-4}$	$2.90313729 \times 10^{-4}$
		7.5	$4.35737112 \times 10^{-4}$	$4.35737112 \times 10^{-4}$	$4.35737112 \times 10^{-4}$

Table 6: Analysis RMSE for different EnKF implementations applied to the QG33 instance. All methods give similar results. When the number of ensemble and/or observations is increased, the analysis accuracy is improved.

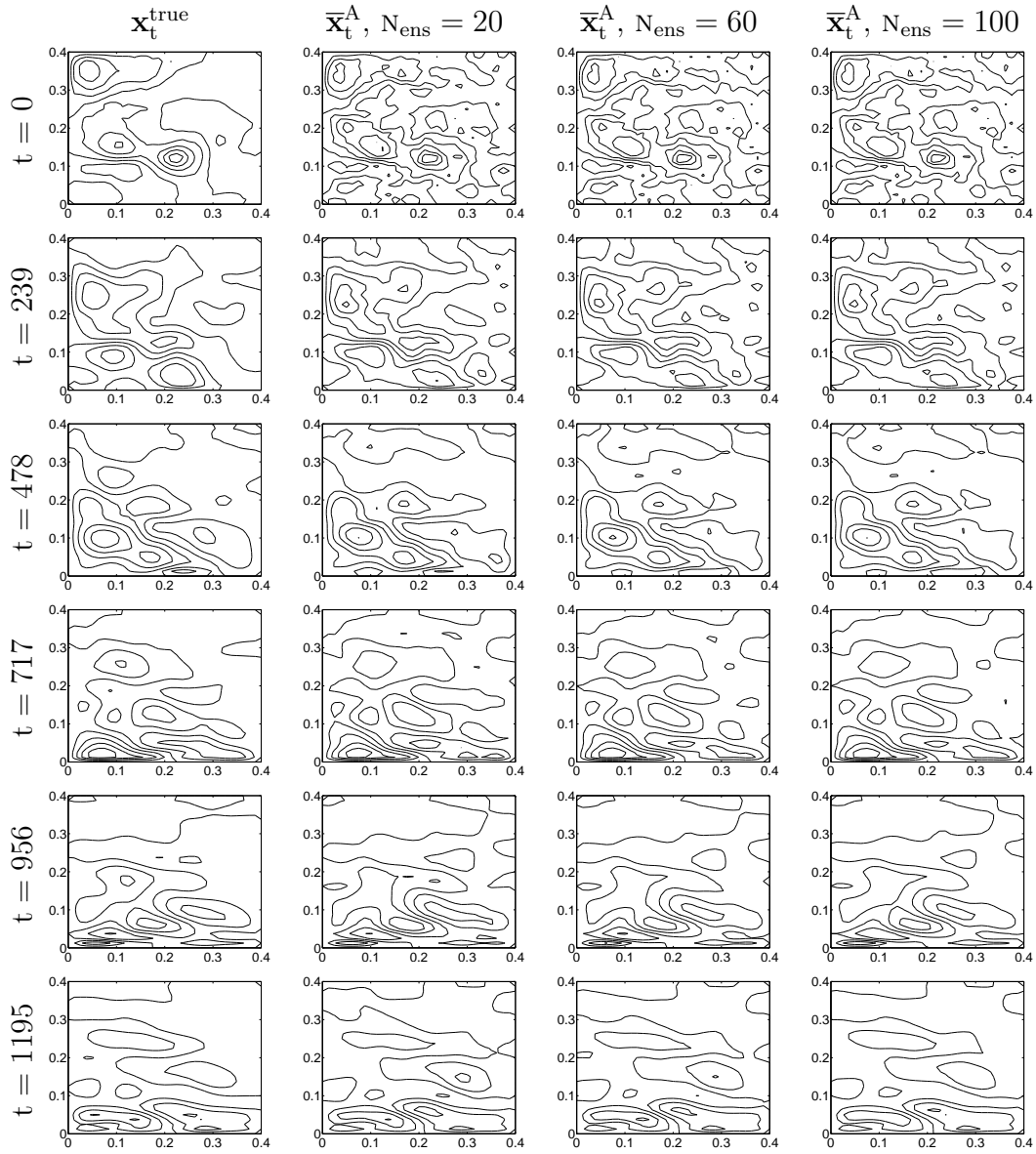


Figure 5: Snapshots of the QG33 simulation for $N_{\text{ens}} = 20, 60$ and 100 members, at the time steps $t = 0, 239, 478, 717, 956$ and 1195 (out of 1200). As expected, when the number of ensemble members is increased the estimation of the true state (\mathbf{x}^{true}) is improved (the RMSE is decreased).

N_{ens}	N_{obs}	STD_{ens}	$EnKF_{Sher}$	$EnKF_{Chol}$	$EnKF_{SVD}$
20	480	2.5	17.6 s	33.4 s	24.7 s
		5.0	17.2 s	32.8 s	25.3 s
		7.5	17.3 s	33.1 s	28.6 s
	672	2.5	17.9 s	61.9 s	39.4 s
		5.0	17.7 s	62.9 s	49.3 s
		7.5	17.8 s	62.1 s	37.6 s
	864	2.5	17.8 s	113.7 s	57.9 s
		5.0	18.2 s	116.3 s	79.7 s
		7.5	18.1 s	118.4 s	61.2 s
60	480	2.5	42.9 s	57.8 s	63.7 s
		5.0	42.9 s	57.5 s	62.9 s
		7.5	42.8 s	57.8 s	58.3 s
	672	2.5	44.3 s	90.3 s	142.3 s
		5.0	44.5 s	89.8 s	92.3 s
		7.5	44.5 s	90.3 s	91.3 s
	864	2.5	46.8 s	150.6 s	187.3 s
		5.0	46.6 s	156.7 s	144.8 s
		7.5	46.5 s	154.3 s	200.9 s
100	480	2.5	72.3 s	83.2 s	102.0 s
		5.0	72.4 s	83.2 s	96.8 s
		7.5	72.6 s	83.4 s	94.4 s
	672	2.5	77.8 s	118.9 s	140.2 s
		5.0	77.8 s	119.5 s	166.8 s
		7.5	77.1 s	120.1 s	216.4 s
	864	2.5	82.8 s	209.1 s	412.9 s
		5.0	83.2 s	212.7 s	289.7 s
		7.5	82.7 s	202.6 s	304.6 s

Table 7: Computational times for several EnKF implementations applied to the QG33 instance. Different numbers of ensemble members and numbers of observations are considered.

N_{ens}	N_{obs}	STD_{ens}	$\text{EnKF}_{\text{Sher}}$	$\text{EnKF}_{\text{Chol}}$	EnKF_{SVD}
20	1984	2.5	$2.38730154 \times 10^{-4}$	$2.38730154 \times 10^{-4}$	$2.38730154 \times 10^{-4}$
		5.0	$4.77366714 \times 10^{-4}$	$4.77366714 \times 10^{-4}$	$4.77366714 \times 10^{-4}$
		7.5	$7.16006328 \times 10^{-4}$	$7.16006328 \times 10^{-4}$	$7.16006328 \times 10^{-4}$
	2778	2.5	$2.38650829 \times 10^{-4}$	$2.38650829 \times 10^{-4}$	$2.38650829 \times 10^{-4}$
		5.0	$4.77195277 \times 10^{-4}$	$4.77195277 \times 10^{-4}$	$4.77195277 \times 10^{-4}$
		7.5	$7.15744082 \times 10^{-4}$	$7.15744082 \times 10^{-4}$	$7.15744082 \times 10^{-4}$
	3572	2.5	$2.38731447 \times 10^{-4}$	$2.38731447 \times 10^{-4}$	$2.38731447 \times 10^{-4}$
		5.0	$4.77279065 \times 10^{-4}$	$4.77279065 \times 10^{-4}$	$4.77279065 \times 10^{-4}$
		7.5	$7.15829932 \times 10^{-4}$	$7.15829932 \times 10^{-4}$	$7.15829932 \times 10^{-4}$
60	1984	2.5	$2.34788461 \times 10^{-4}$	$2.34788461 \times 10^{-4}$	$2.34788461 \times 10^{-4}$
		5.0	$4.69640125 \times 10^{-4}$	$4.69640125 \times 10^{-4}$	$4.69640125 \times 10^{-4}$
		7.5	$7.04505865 \times 10^{-4}$	$7.04505865 \times 10^{-4}$	$7.04505865 \times 10^{-4}$
	2778	2.5	$2.34427724 \times 10^{-4}$	$2.34427724 \times 10^{-4}$	$2.34427724 \times 10^{-4}$
		5.0	$4.68838293 \times 10^{-4}$	$4.68838293 \times 10^{-4}$	$4.68838293 \times 10^{-4}$
		7.5	$7.03254635 \times 10^{-4}$	$7.03254635 \times 10^{-4}$	$7.03254635 \times 10^{-4}$
	3572	2.5	$2.34303497 \times 10^{-4}$	$2.34303497 \times 10^{-4}$	$2.34303497 \times 10^{-4}$
		5.0	$4.68673565 \times 10^{-4}$	$4.68673565 \times 10^{-4}$	$4.68673565 \times 10^{-4}$
		7.5	$7.03046901 \times 10^{-4}$	$7.03046901 \times 10^{-4}$	$7.03046901 \times 10^{-4}$
100	1984	2.5	$2.37123911 \times 10^{-4}$	$2.37123911 \times 10^{-4}$	$2.37123911 \times 10^{-4}$
		5.0	$4.74051478 \times 10^{-4}$	$4.74051478 \times 10^{-4}$	$4.74051478 \times 10^{-4}$
		7.5	$7.10951271 \times 10^{-4}$	$7.10951271 \times 10^{-4}$	$7.10951271 \times 10^{-4}$
	2778	2.5	$2.34083117 \times 10^{-4}$	$2.34083117 \times 10^{-4}$	$2.34083117 \times 10^{-4}$
		5.0	$4.68257831 \times 10^{-4}$	$4.68257831 \times 10^{-4}$	$4.68257831 \times 10^{-4}$
		7.5	$7.02424460 \times 10^{-4}$	$7.02424460 \times 10^{-4}$	$7.02424460 \times 10^{-4}$
	3572	2.5	$2.32378928 \times 10^{-4}$	$2.32378928 \times 10^{-4}$	$2.32378928 \times 10^{-4}$
		5.0	$4.64697670 \times 10^{-4}$	$4.64697670 \times 10^{-4}$	$4.64697670 \times 10^{-4}$
		7.5	$6.97023351 \times 10^{-4}$	$6.97023351 \times 10^{-4}$	$6.97023351 \times 10^{-4}$

Table 8: Analysis RMSE for different EnKF implementations applied to the QG65 instance. All methods give similar results.

N_{ens}	N_{obs}	STD_{ens}	$EnKF_{Sher}$	$EnKF_{Chol}$	$EnKF_{SVD}$
20	1984	2.5	71.5 s	44.9 min	454.7 s
		5.0	70.6 s	33.4 min	429.3 s
		7.5	70.3 s	45.4 min	360.6 s
	2778	2.5	71.0 s	1.8 h	831.1 s
		5.0	73.2 s	1.3 h	735.7 s
		7.5	71.9 s	1.4 h	795.8 s
	3572	2.5	72.2 s	3.8 h	1602.5 s
		5.0	74.3 s	3.3 h	1112.3 s
		7.5	72.2 s	3.0 h	771.5 s
60	1984	2.5	179.0 s	45.0 min	1215.7 s
		5.0	179.5 s	55.3 min	1235.6 s
		7.5	178.4 s	51.9 min	1066.7 s
	2778	2.5	190.6 s	2.4 h	1463.3 s
		5.0	188.3 s	1.9 h	39.4 min
		7.5	189.7 s	2.5 h	32.4 min
	3572	2.5	202.6 s	4.1 h	1.2 h
		5.0	198.9 s	2.9 h	1.1 h
		7.5	201.9 s	4.3 h	1.0 h
100	1984	2.5	313.8 s	52.4 min	37.2 min
		5.0	314.3 s	40.1 min	33.2 min
		7.5	309.6 s	58.4 min	37.9 min
	2778	2.5	346.9 s	1.7 h	1.1 h
		5.0	342.9 s	1.7 h	1.0 h
		7.5	340.7 s	2.9 h	1.1 h
	3572	2.5	373.9 s	4.8 h	1.6 h
		5.0	378.3 s	4.0 h	1.8 h
		7.5	383.7 s	5.1 h	1.3 h

Table 9: Computational times for several EnKF implementations applied to the QG65 instance. Different numbers of ensemble members and numbers of observations are considered.

N_{ens}	N_{obs}	STD_{ens}	$\text{EnKF}_{\text{Sher}}$	EnKF_{SVD}
20	8064	2.5	$9.92105438 \times 10^{-5}$	$9.92105438 \times 10^{-5}$
		5.0	$1.98414661 \times 10^{-4}$	$1.98414661 \times 10^{-4}$
		7.5	$2.97618537 \times 10^{-4}$	$2.97618537 \times 10^{-4}$
	11290	2.5	$9.90045121 \times 10^{-5}$	$9.90045121 \times 10^{-5}$
		5.0	$1.97996616 \times 10^{-4}$	$1.97996616 \times 10^{-4}$
		7.5	$2.96988644 \times 10^{-4}$	$2.96988644 \times 10^{-4}$
	14516	2.5	$9.87990386 \times 10^{-5}$	$9.87990386 \times 10^{-5}$
		5.0	$1.97591049 \times 10^{-4}$	$1.97591049 \times 10^{-4}$
		7.5	$2.96383002 \times 10^{-4}$	$2.96383002 \times 10^{-4}$
60	8064	2.5	$9.74245572 \times 10^{-5}$	$9.74245572 \times 10^{-5}$
		5.0	$1.94820830 \times 10^{-4}$	$1.94820830 \times 10^{-4}$
		7.5	$2.92217500 \times 10^{-4}$	$2.92217500 \times 10^{-4}$
	11290	2.5	$9.63593685 \times 10^{-5}$	$9.63593685 \times 10^{-5}$
		5.0	$1.92682256 \times 10^{-4}$	$1.92682256 \times 10^{-4}$
		7.5	$2.89005780 \times 10^{-4}$	$2.89005780 \times 10^{-4}$
	14516	2.5	$9.67669396 \times 10^{-5}$	$9.67669396 \times 10^{-5}$
		5.0	$1.93545013 \times 10^{-4}$	$1.93545013 \times 10^{-4}$
		7.5	$2.90322987 \times 10^{-4}$	$2.90322987 \times 10^{-4}$
100	8064	2.5	$9.56333807 \times 10^{-5}$	$9.56333807 \times 10^{-5}$
		5.0	$1.91331921 \times 10^{-4}$	$1.91331921 \times 10^{-4}$
		7.5	$2.87027307 \times 10^{-4}$	$2.87027307 \times 10^{-4}$
	11290	2.5	$9.49419202 \times 10^{-5}$	$9.49419202 \times 10^{-5}$
		5.0	$1.89929524 \times 10^{-4}$	$1.89929524 \times 10^{-4}$
		7.5	$2.84918006 \times 10^{-4}$	$2.84918006 \times 10^{-4}$
	14516	2.5	$9.47165868 \times 10^{-5}$	$9.47165868 \times 10^{-5}$
		5.0	$1.89427095 \times 10^{-4}$	$1.89427095 \times 10^{-4}$
		7.5	$2.84137686 \times 10^{-4}$	$2.84137686 \times 10^{-4}$

Table 10: Analysis RMSE for different EnKF implementations applied to the QG129 instance. All methods give similar results.

N_{ens}	N_{obs}	STD_{ens}	$\text{EnKF}_{\text{Sher}}$	EnKF_{SVD}
20	8064	5	289.9 s	1.8 h
		5.0	293.5 s	1.4 h
		7.5	286.8 s	1.9 h
	11290	5	303.2 s	2.2 h
		5.0	302.2 s	2.0 h
		7.5	303.5 s	2.9 h
	14516	5	315.7 s	4.5 h
		5.0	308.1 s	3.8 h
		7.5	309.1 s	3.7 h
60	8064	5	764.8 s	4.1 h
		5.0	795.9 s	3.2 h
		7.5	764.7 s	3.9 h
	11290	5	838.0 s	6.3 h
		5.0	832.6 s	5.4 h
		7.5	817.7 s	6.7 h
	14516	5	910.7 s	9.9 h
		5.0	899.9 s	9.3 h
		7.5	864.8 s	11.2 h
100	8064	5	1381.5 s	5.3 h
		5.0	1360.3 s	5.2 h
		7.5	1397.9 s	5.9 h
	11290	5	1492.4 s	10.3 h
		5.0	1494.5 s	8.9 h
		7.5	1506.6 s	6.7 h
	14516	5	1624.8 s	13.7 h
		5.0	1634.9 s	12.9 h
		7.5	1664.2 s	14.9 h

Table 11: Computational times for several EnKF implementations applied to the QG129 instance. Different numbers of ensemble members and numbers of observations are considered.

5 Conclusions and Future Work

We propose a novel implementation of the EnKF based on an iterative application of the Sherman-Morrison formula. The algorithm exploits the special structure of the background error covariance matrix projected onto the observation space. The computational complexity of the new approach is equivalent to that of the best EnKF implementations available in the literature. Nevertheless, the performance (elapsed time) of most of the existing methods is strongly dependent from the condition $N_{\text{obs}} \gg N_{\text{ens}}$ (the number of observations is large compared to the ensemble size); the performance of the new approach is not affected by this condition. In addition, the

term N_{ens}^3 is not presented in the upper-bound of the effort of the proposed method, which leads to better performance when the number of observations and of ensemble members are of similar magnitude ($N_{\text{obs}} \sim N_{\text{ens}}$). A sufficient condition for the stability of the proposed method is the non-singularity of the data error covariance matrix, which, in practice, is always the case. In addition, a pivoting strategy is developed in order to reduce round-off error propagation without increasing the computational effort of the proposed method. The computational cost of this algorithm provides a better theoretical performance than other generic formulations of matrix inversion based on the Sherman Morrison formula available in the literature. To assess the accuracy and performance of the proposed implementation two standard test problems have been employed, namely, the Lorenz 96 and the quasi-geostrophic models. All EnKF implementations tested (Cholesky, SVD, Sherman-Morrison) provide virtually identical analyses. However, the proposed Sherman-Morrison approach is much faster than the others even when the number of observations is large with respect to the number of ensemble members ($N_{\text{obs}} \gg N_{\text{ens}}$). The parallel version of the new algorithm has a theoretical complexity that grows only linearly with the number of observations, and is therefore well suited for implementation in large scale data assimilation systems.

Acknowledgment

This work has been supported in part by NSF through awards NSF OCI-8670904397, NSF CCF-0916493, NSF DMS-0915047, NSF CMMI-1130667, NSF CCF-1218454, AFOSR FA9550-12-1-0293-DEF, AFOSR 12-2640-06, and by the Computational Science Laboratory at Virginia Tech.

References

- [1] E. Anderson, Z. Bai, J. Dongarra, A. Greenbaum, A. McKenney, J. Du Croz, S. Hammerling, J. Demmel, C. Bischof, and D. Sorensen. Lapack: A portable linear algebra library for high-performance computers. In *Proceedings of the 1990 ACM/IEEE conference on Supercomputing*, Supercomputing 90, pages 2–11, Los Alamitos, CA, USA, 1990. IEEE Computer Society Press.
- [2] J. L. Anderson. An Ensemble Adjustment Kalman Filter for Data Assimilation. *Monthly Weather Review*, 2001.

- [3] J. L. Anderson. Exploring the need for localization in ensemble data assimilation using a hierarchical ensemble filter. *Physica D: Nonlinear Phenomena*, 230(1–2):99 – 111, 2007.
- [4] J. L. Anderson and N. Collins. Scalable Implementations of Ensemble Filter Algorithms for Data Assimilation. *Journal of Atmospheric & Oceanic Technology*, 2007.
- [5] X. Carton and R. Baraille. Data Assimilation in Quasi-geostrophic Ocean Models. In *OCEANS 94. Oceans Engineering for Today’s Technology and Tomorrow’s Preservation. Proceedings*, volume 3, pages III/337 –III/346 vol.3, sep 1994.
- [6] A. Cohen. Rate of Convergence of Several Conjugate Gradient Algorithms. *SIAM Journal on Numerical Analysis*, 9(2):248–259, 1972.
- [7] S. Eisenstat. Efficient Implementation of a Class of Preconditioned Conjugate Gradient Methods. *SIAM Journal on Scientific and Statistical Computing*, 2(1):1–4, 1981.
- [8] G. Evensen. *Data Assimilation: The Ensemble Kalman Filter*, chapter 14, pages 210–237. Springer, 2009.
- [9] G. Evensen. Estimation in an oil reservoir simulator. In *Data Assimilation*, pages 263–272. Springer Berlin Heidelberg, 2009.
- [10] G. Evensen. The Ensemble Kalman Filter for Combined State and Parameter Estimation. *Control Systems, IEEE*, 29(3):83 –104, june 2009.
- [11] A. M. Fraser. *Appendix A: Formulas for Matrices and Gaussians*, chapter 7, pages 117–120. SIAM, 2008.
- [12] P. Gill, M. Saunders, and J. Shinnerl. On the Stability of Cholesky Factorization for Symmetric Quasidefinite Systems. *SIAM Journal on Matrix Analysis and Applications*, 17(1):35–46, 1996.
- [13] G. Golub and D. OLeary. Some History of the Conjugate Gradient and Lanczos Algorithms: 1948-1976. *SIAM Review*, 31(1):50–102, 1989.
- [14] V. Haugen, G. Naevdal, L. J. Natvik, G. Evensen, A. Berg, and K. Flornes. History Matching Using the Ensemble Kalman Filter on a North Sea Field Case. *SPE Journal*, 13:382–391, 2008.

- [15] A. Kovalenko, T. Mannseth, and G. Nævdal. Error Estimate for the Ensemble Kalman Filter Analysis Step. *SIAM Journal on Matrix Analysis and Applications*, 32(4):1275–1287, 2011.
- [16] H. Li, E. Kalnay, and T. Miyoshi. Simultaneous Estimation of Covariance Inflation and Observation Errors within an Ensemble Kalman Filter. *Quarterly Journal of the Royal Meteorological Society*, 135(639):523–533, 2009.
- [17] C. Lin and J. More. Incomplete Cholesky Factorizations with Limited Memory. *SIAM Journal on Scientific Computing*, 21(1):24–45, 1999.
- [18] E. N. Lorenz and K. A. Emanuel. Optimal sites for supplementary weather observations: Simulation with a small model. *Journal of the Atmospheric Sciences*, 1998.
- [19] J. Mandel. Efficient Implementation of the Ensemble Kalman Filter . Technical report, University of Colorado at Denver and Health Sciences Center, 2006.
- [20] P. Maponi. The solution of linear systems by using the sherman–morrison formula. *Linear Algebra and its Applications*, 420(2–3):276 – 294, 2007.
- [21] J. Meinguet. Refined Error Analyses of Cholesky Factorization. *SIAM Journal on Numerical Analysis*, 20(6):1243–1250, 1983.
- [22] E. Ott, B. R. Hunt, I. Szunyogh, A. V. Zimin, E. J. Kostelich, M. Corazza, E. Kalnay, D. J. Patil, and J. A. Yorke. A Local Ensemble Kalman Filter for Atmospheric Data Assimilation. *Tellus A*, 56(5):415–428, 2004.
- [23] K. Otto and E. Larsson. Iterative Solution of the Helmholtz Equation by a Second-Order Method. *SIAM Journal on Matrix Analysis and Applications*, 21(1):209–229, 1999.
- [24] J. Pedlosky. *Geophysical Fluids Dynamics*. Springer-Verlag, New York Heidelberg, 1996.
- [25] J. Reid. The Use of Conjugate Gradients for Systems of Linear Equations Possessing Property A. *SIAM Journal on Numerical Analysis*, 9(2):325–332, 1972.
- [26] R. Schnabel and E. Eskow. A New Modified Cholesky Factorization. *SIAM Journal on Scientific and Statistical Computing*, 11(6):1136–1158, 1990.

- [27] M. Stewart and P. Van Dooren. Stability Issues in the Factorization of Structured Matrices. *SIAM Journal on Matrix Analysis and Applications*, 18(1):104–118, 1997.
- [28] A. Suarez, R. Heather Dawn, W. Dustan, and M. Coniglio. Comparison Of Ensemble Kalman Filter–based Forecasts to Traditional Ensemble and Deterministic Forecasts for a Case Study of Banded Snow. *Weather and Forecasting*, 27:85–105, 2012.
- [29] M. K. Tippett, J. L. Anderson, C. H. Bishop, T. M. Hamill, and J. S. Whitaker. Ensemble Square Root Filters. *Monthly Weather Review*, 2003.
- [30] G. Wu, X. Zheng, and Y. Li. Inflation Adjustment on Error Covariance Matrix of Ensemble Kalman Filter. In *Multimedia Technology (ICMT), 2011 International Conference on*, pages 2160 –2163, july 2011.
- [31] J. Xia and M. Gu. Robust Approximate Cholesky Factorization of Rank-Structured Symmetric Positive Definite Matrices. *SIAM Journal on Matrix Analysis and Applications*, 31(5):2899–2920, 2010.